7-1-1967

Dynamic Behavior Due to an Eccentrically Applied Lateral Vibration of a Model Bridge With Rigid and Elastomeric Bearings

Subhas Kumar Bose

DYNAMIC BEHAVIOR DUE TO AN ECCENTRICALLY APPLIED LATERAL VIBRATION OF A MODEL BRIDGE WITH RIGID AND ELASTOMERIC BEARINGS

by

Subhas Kumar Bose
B.E. in Department of Civil Engineering
Jadavpur University, Calcutta, India, 1963

A Thesis
Submitted to the Faculty
of the
University of North Dakota
in partial fulfillment of the requirements
for the Degree of
Master of Science

Grand Forks, North Dakota
July
1967

This thesis submitted by Subhas Kumar Bose in partial fulfillment of the requirements for the Degree of Master of Science in the University of North Dakota is hereby approved by the Committee under whom the work has been done.

Jack H. Emanuel
Chairman

Irvin R. Jensen

Oscar E Manz

Albert E. Anuta J.

William Johnson
Dean of the Graduate School

ACKNOWLEDGMENTS

The author wishes to express his sincere appreciation to Dr. Jack H. Emanuel, his Graduate Committee Chairman, for his generous help, patience and enthusiastic guidance in this investigation and also for his friendship and counsel.

Appreciation is also extended to Professors Ivan R. Jensen, Oscar E. Manz and Albert E. Anuta, Jr. for their assistance and constructive criticism.

The author also wishes to thank Mrs. Jack H. Emanuel for her continued encouragement.

CONTENTS

LIST OF TABLES

LIST OF FIGURES

ABSTRACT

In this investigation a comparative study is made of the dynamic behavior of rigid and elastomeric bearings of a model bridge subjected to eccentric vibratory loading.

For the experimental portion, static and vibration tests were conducted using an approximate one-third scale model bridge 25 ft long and 10 ft wide, with a composite section of steel girders and concrete bridge deck slab. A counterrotating eccentric weight oscillator was used to produce oscillatory loads on the bridge. Tests were conducted with three types of bearing conditions: curved steel sole plates, 64 durometer and 49 durometer hardness neoprene pads.

A theoretical analysis was also made and the values obtained for natural frequencies and deflections were compared with those obtained experimentally.

Some of the conclusions are: (a) for a statically applied load the total midspan deflection is greater for neoprene than steel supports; (b) neoprene bearing pads add to the damping of the bridge; (c) in general, though not always, the maximum strain and also the total and the net deflection in the girders, at the respective natural frequency for each bearing condition, are greater for steel bearings; (d) the dynamic stress and deflection, and also their amplification

factors, of a loaded bridge are less than those of an unloaded bridge; (e) at low and high frequencies the magnitudes of strain and deflection are quite close for different bearing conditions.

INTRODUCTION

Field observations of short span highway bridges reveal a wide variety of types of bridge supporting and expansion devices used. Bridge supporting devices, which have been and are currently being used, vary from elaborate roller nests to cast or welded rockers, self lubricating bronze plates, curved steel plates, flat steel plates and simple elastomeric pads. Each type is subject to limitations and possible inconsistencies of behavior.

One investigator has indicated that either of two relatively simple and economical types of supporting devices might be used to eliminate many of the problems associated with most devices currently used (3). One of these types is elastomeric bearings. Another investigator has indicated some possible benefits in the dynamic behavior of bridges through the use of elastomeric bearings (20).

The use of elastomeric pads is comparatively new in the United States, and they have been used primarily for prestressed concrete bridges. However, in some European countries they have been extensively used for some time. Elastomeric pads were widely used in France to rebuild bridges which were destroyed during World War II. In the

discussion of "Elastomeric Bridge Bearings", by Pare and Keiner (13), McCready (10) stated that the Freysinett Company, pioneers in prestressed concrete, did a lot of original work on the subject. According to the same author, the English also are using elastomeric bridge pads and they too have developed engineering data on the subject.

Neoprene pads were used for several bridges in Ontario, Canada, and their behavior under extreme winter periods has been quite satisfactory.(10).

Some investigators have concluded that the use of elastomeric pads is also quite practicable in the United States (12, 13). However, other engineers believe that further studies should be conducted on the behavior of elastomeric pads.

"Elastomer" is a very broad term which includes all materials that exhibit rubber-like properties. At the present time neoprene appears to have the best combination of the required properties of the elastomers available.

An experimental comparison of the dynamic behavior of a model bridge with rigid and elastomeric (neoprene) bearings, and subjected to an oscillating load at the mid-point has been completed (3). During that investigation data were also taken for the dynamic behavior due to an off-center, or eccentric, oscillatory loading. This data was not reduced, nor was an analytical comparison made.

It is believed that the results of the uncompleted portion of the above investigation would be of benefit to bridge design engineers. Therefore, this project was initiated to utilize that data and further study whether beneficial dynamic behavior is obtained by use of elastomeric bearings.

REVIEW OF LITERATURE

A review of available literature is helpful in recognition of the problem.

Contrasting the behavior of bridges with rigid and elastomeric bearings, Zuk (20) concluded that when elastomeric bearings are used:

(1) the dynamic deflections are increased;

(2) the natural frequency of vibration is reduced;

(3) the elastomeric bearings add damping to the system; and

(4) the dynamic stresses in the bridges are significantly reduced.

If dynamic stresses are reduced when elastomeric bearings are used, structural economy would result.

Dynamic stresses result from the application of a time-dependent forcing function. Several factors influence the forcing functions. These include the effects of roughness of floors, spring action of a vehicle, and oscillations produced by repetition of axles across any point. These effects and/or the combination of them have been investigated by several investigators (1, 2, 4, 5, 9, 14, 16, 18, 19). In general their conclusions consider the basis for the present AASHO Specifications to be unrealistic.

Highway Research Board Bulletin 124 gives a good collection of papers on the subject of highway bridge vibrations. In this bulletin, Biggs and Suer (1) observed that the most important single factor influencing the amplitude of vibration is the vertical oscillation of the vehicle as it approaches the span. Scheffey (14) investigated the significance of the various dynamic effects on the vibration of highway bridges. In a comparison of measured deflections and stresses in two continuous plate girder bridges, Edgerton and Beecroft (2) reported that the observed stresses were lower than the stresses calculated on the basis of AASHO specifications, except in the case of the unloaded girder under eccentric loading. Hayes and Sbarounis (5) studied the effect of load and composite beam action on the natural frequency of a three-span continuous I-beam bridge. Foster and Oehler (4) attempted to correlate the dynamic deflection with the stringer depth to span ratio for a number of simple span roller-beam and plate-girder bridges. A review of analytical and experimental research at the University of Illinois on the problem of highway bridge impact was presented by Tung, Goodman, Chen and Newmark (18).

A theoretical study of and experimental data relating to the dynamic response due to moving loads of a deck steel girder continuous bridge was presented by Wise (19). The tests indicated that the AASHO impact factor formula tended

to overestimate the impact effect by about fifty per cent. A tentative impact formula was suggested.

A large number of bridges were tested to study the dynamic effects produced under moving vehicles, and to relate the observed behavior to the results predicted by theory (6).

Senne investigated the distribution of single loads (static) on two laboratory test bridges and two full size highway simple span bridges, and two four span continuous highway bridges. In this investigation torsion was neglected, but it is suggested that torsion could be taken into account in the proposed method by including energy expressions for torsion as well as moment (15).

Linger and Hulsbos (9) attempted to correlate the response of actual continuous highway bridges under the effects of moving vehicles with vibration theory.

One investigator utilized model trucks and an oscillator to induce vibration of a model bridge (16). The same model bridge subjected to oscillatory loading was used for a comparative study of the dynamic behavior of rigid and elastomeric bearings (3).

EXPERIMENTAL INVESTIGATION

The model bridge shown in Fig. 1 was used by Emanuel (3) to study the comparative vibrational behavior of rigid and elastomeric bearings. Properties of the test bridge and the instrumentation are given in the report of that investigation. Only the more important features pertinent to this study are described in this report.

Test Bridge

The model bridge was built approximately to a one-third scale with a length of 25 ft and a roadway of 10 ft. However, it cannot be called an exact geometric model due to some changes made for experimental purposes.

The deck is a 2¼-in. concrete slab. The primary reinforcement consists of No. 5 smooth wires (0.207 in.-diameter) spaced at 2 in. centers. Two of every three wires are bent up over the supports for negative reinforcing, and an additional wire is located near the top of the slab above the third rod. Number 5 wires spaced at 7.7 in. on center and near the bottom constitute the longitudinal reinforcement. Coverage used is 7/16 in. to the center of the primary reinforcement at both faces. Shear lugs were welded to the top of the beams to insure composite action between steel and concrete.

Fig. 1. Test bridge

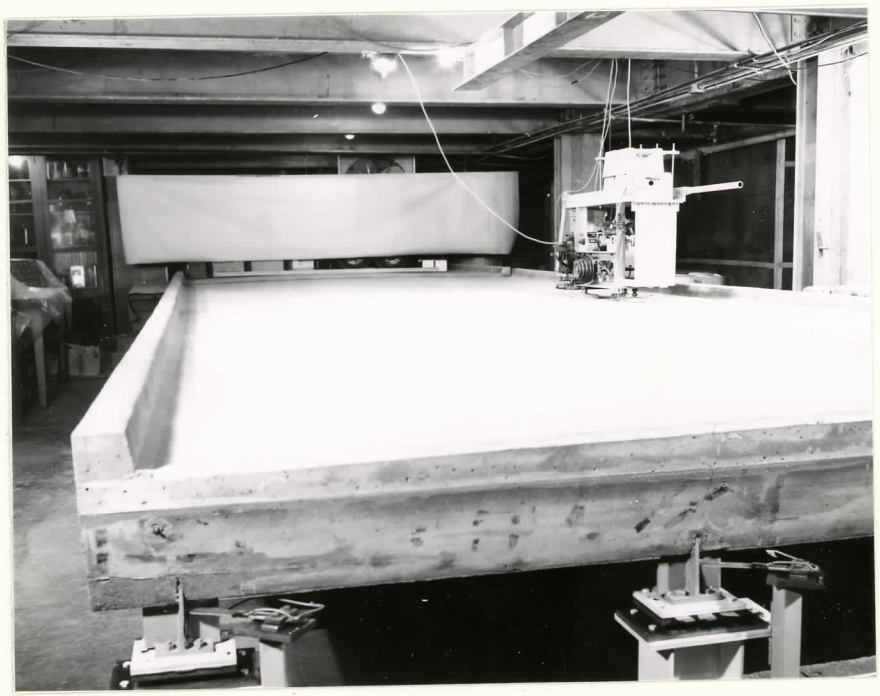

General details of the bridge are shown in Fig. 2 and pertinent bridge properties are given in Table 1.

Instrumentation

The instrumentation was designed to determine the strains and vertical displacements of the steel girders for dynamic loading at different frequencies. These tests were repeated for three bearing conditions.

Strains were measured at midspan of the girders and deflections were measured at midspan and supports. Measurements were made by means of Type A-1, SR-4 electric wire resistance gages. Equipment used for recording strain and deflection data included eight Model BL-520 Brush Universal amplifiers with Model BL-350 strain gage input boxes; two Model BL-274 Brush four channel oscillographs; and three 20 channel and one 6 channel Baldwin SR-4 bridge balancing units (Fig. 3). One Baldwin-Lima-Hamilton Type N, SR-4 strain indicator; one Baldwin SR-4 load cell, Type C, 20,000 lb capacity; and one Blackhawk 10-ton hydraulic Porto-Power unit were also used for static load tests.

One oscillograph and four of the amplifiers were used for recording strains at midspan of each beam. To record deflections the other four amplifiers and oscillograph were used with the four bridge balancing units so that either midspan deflections or end deflections at either end of all four beams or midspan and end deflections of individual

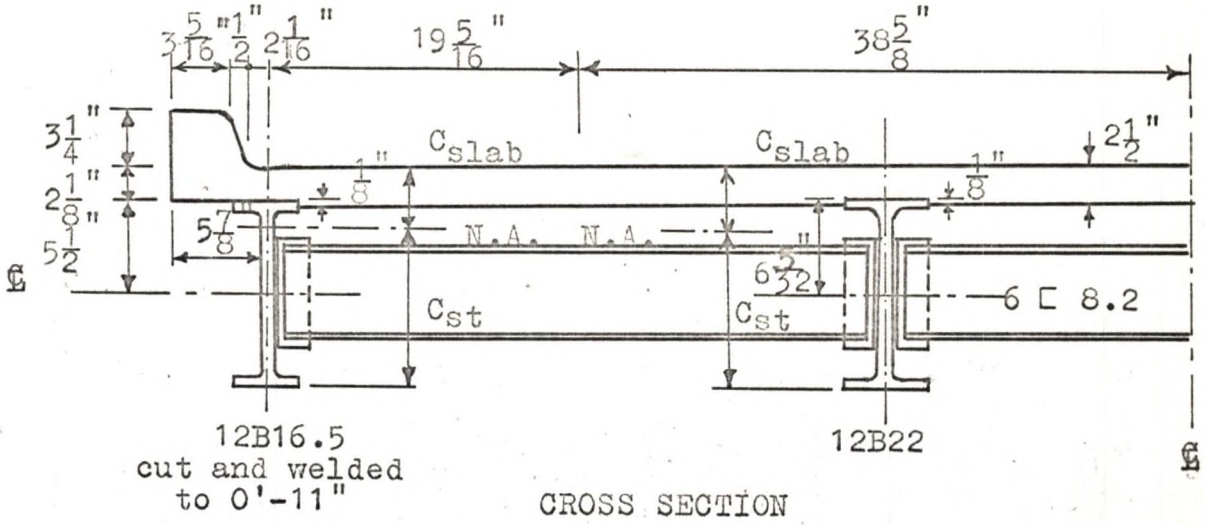

CROSS SECTION

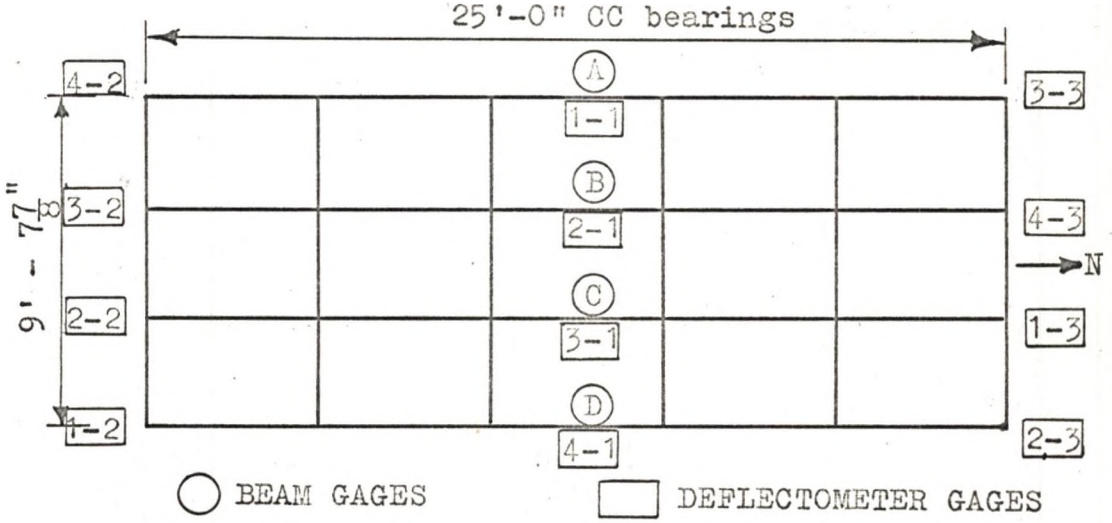

STRAIN GAGE LOCATION

Fig. 2. General details of test bridge

TABLE 1

PROPERTIES OF TEST BRIDGE[a]

Span (L), ft	25	
Roadway width, ft	10	
Beam spacing (S), ft	3.22	
Slab thickness, in.	2.25	
Ratio $I_{int.}/I_{ext.}$ at midspan[b]	1.48	
EI of total section[c] at midspan, $(10)^9$ lb-in.^{2}	37.43	
Total weight of bridge[d], lb	11,031	
	Interior Beam	Exterior Beam
I of beam[c] at midspan, in.^{4}	379	256
EI of beam[c] at midspan, $(10)^9$ lb-in.^{2}	11.14	7.52
I_{st}/c_{st} at midspan, in.^{3}	35.8	25.9
I of beam[e] at midspan, in.^{4}	3030	2047
c_{slab}, in.	3.87	3.25
c_{st}, in.	10.57	9.88
Area of beam, sq in.	6.75	5.01
Area of concrete, sq in.	86.9	67.6
Weight of beam, plf	22.0	16.5
Weight of concrete, plf	90.5	70.5

[a] From Emanuel (3, p. 44)

[b] Composite interior and exterior beams

[c] Equivalent all-steel section, n = 8

[d] Experimentally determined, this research

[e] Equivalent all-concrete section

Fig. 3. Recording equipment

beams could be recorded at one time. Strain gage locations are shown in Fig. 2.

Oscillator

A counterrotating eccentric weight oscillator, or exciter, was used to produce the oscillating loads on the bridge. The horizontal components of the force cancel each other and vertical components are additive.

The vertical driving force F, in pounds, produced for equal weights and eccentricities is given by the equation (11, p. 51)

$$F = \frac{2We}{g}\omega^2 \qquad (1)$$

where,

w = weight of each rotating mass, lb--3.48 lb for the data reduced in this investigation

e = eccentricity of the mass center of each weight, --3.26 in. for the data reduced in this investigation

g = acceleration due to gravity, in./sec^2

ω = rotational velocity, rad/sec

The oscillator was operated by a one-horsepower variable speed motor. The eccentric weights were threaded on shafts so that the eccentricity could be varied. Locking screws were provided to prevent slipping during operation. Total weight of the oscillator was 644 lb.

During the experiment the frequency of the forcing function was varied. It was found that as the forcing function

approached the natural frequency of the bridge, any attempt to increase, or decrease as the case might be, the speed of the motor resulted only in a larger amplitude of deflection. Then the frequency of the forcing function "slipped" past the natural frequency and leveled off at about 1½ to 2 cycles per second beyond the natural frequency. Ku (8, p. 161) explains a similar jump phenomenon for nonlinear systems subjected to a forcing function.

Bridge Bearings

The three types of bearings used consisted of curved steel sole plates, 64 durometer hardness neoprene pads, and 49 durometer hardness neoprene pads (Fig. 4).

The curved steel sole plates were made of 7/8 by 2½ by 4 in. cold-rolled steel turned to a 5½-in. radius in the 2½-in. dimension and welded to ½ by 5½ by 7 in. blocking plates. Bearing (masonry) plates were ½ by 6 by 10 in. hot rolled steel and contact surfaces were milled. The plates had a finish finer than ASA-125 required by some State Highway Departments. Two ½-in. tapered pintles were mounted in each bearing plate. Two 37/64-in. holes were drilled in the curved steel sole plates at the fixed end and slotted holes 19/32 by 3/4-in. were used at the expansion end.

The neoprene pads were furnished by the General Tire and Rubber Co., and had an average size of 4 by 3½ by 0.660 in. The 3½ in. dimension was placed in the longitudinal

Fig. 4. Curved steel sole plate, bearing (masonry) plate, and neoprene pads

direction of the girders. Average shape factor was 1.41. The properties of the neoprene pads are given in Table 2 and stress-deflection curves are shown in Fig. 5.

TABLE 2

PROPERTIES OF NEOPRENE PADS[a]

	64 durometer	49 durometer
Spring modulus, lb/in.		
at 715 psi	69,000	57,100
at 250 psi	64,800	41,400
at 100 psi	64,800	35,000
Natural frequency, cps		
using d at 715 psi	8.3	7.5
using d at 250 psi	13.5	10.8
using d at 100 psi	21.3	15.7
Compressive strain, per cent		
at 715 psi	21.9	26.8
at 250 psi	8.2	12.9
at 100 psi	3.3	6.1

[a]From Emanuel (3, p. 58)

Testing Procedure

The same testing procedure was adopted for the three types of bearing conditions in the following order: (1) curved steel sole plates; (2) 49 durometer neoprene pads;

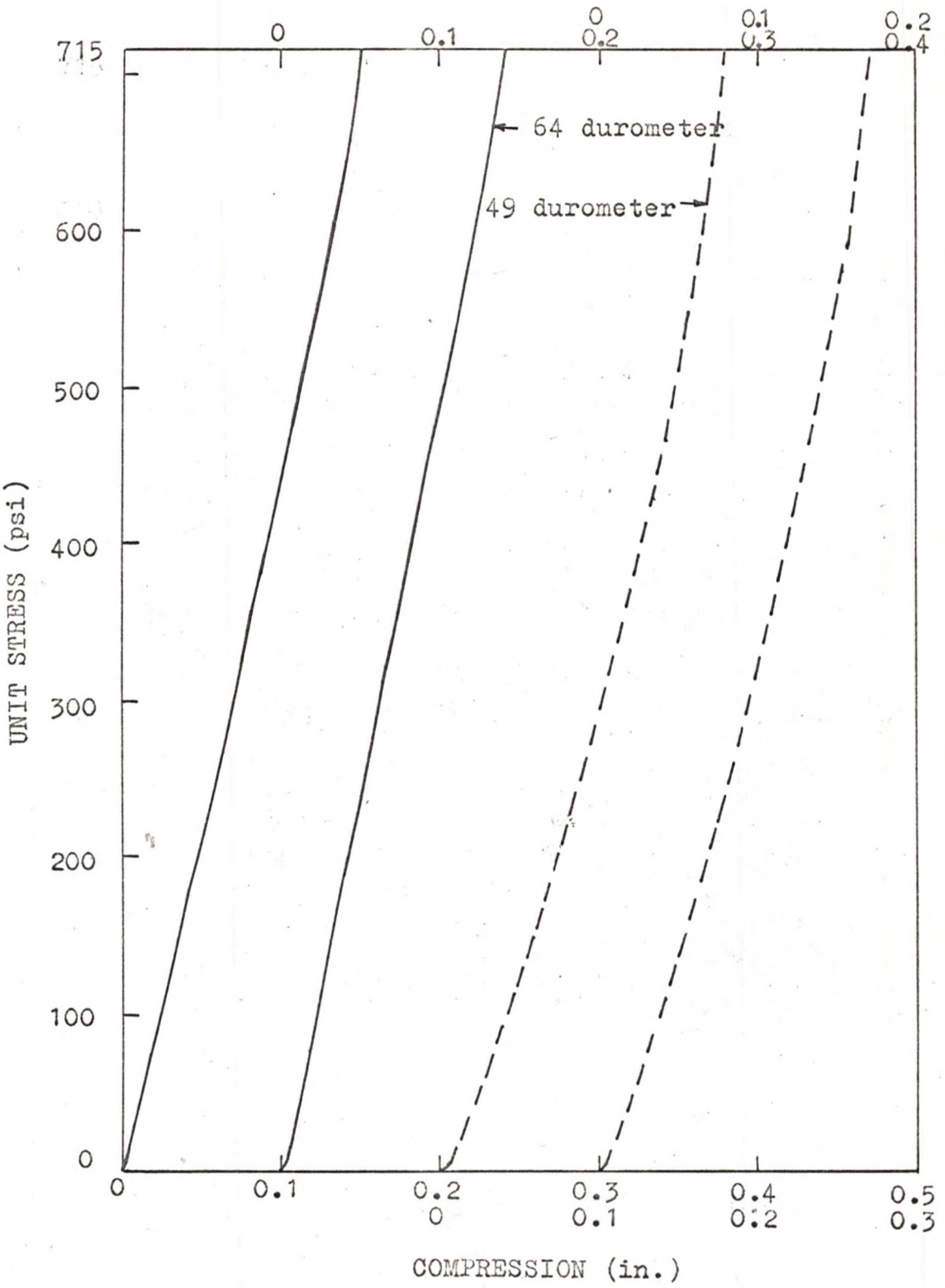

Fig. 5. Stress-deflection curves for neoprene pads

and (3) 64 durometer neoprene pads. A complete series of static load, natural frequency and forced vibration tests was completed for each type of bearing condition.

After each set of tests, the bridge was jacked up and bearings were changed. To assure the same reactions for each type of bearing, shims were inserted between the blocking plates to give the same relative distance in each case from the bottom flange to the reference points. Some creep was encountered when shiming for neoprene pads.

Static Load Tests

Static load tests were conducted to obtain calibration curves for reduction of data. Approximate maximum downward loading of 4000 lb and upward loading of 3000 lb was applied. The tests were repeated for the three bearing conditions.

Natural Frequency

The method of obtaining free vibration was to have a person jump on the bridge and lift his feet instantaneously. Tests were made with the oscillator placed near one side and at midspan of the bridge. The data were reduced from oscillograph recordings of strain and deflection at midspan. Natural frequencies of the bridge with concrete blocks placed alongside the oscillator were also found for the three types of bearings.

Forced Vibration Tests

The oscillator was placed on the east side of the bridge (Figs. 1 and 2) and a series of constant and variable frequency tests were conducted. For the variable frequency tests, the frequency was slowly increased from about 4 cps to the natural frequency and then decreased from about 12 cps to the natural frequency.

Tests were also conducted with 1576 lb of concrete blocks placed alongside the oscillator (Fig. 6).

Fig. 6. Oscillator with concrete blocks

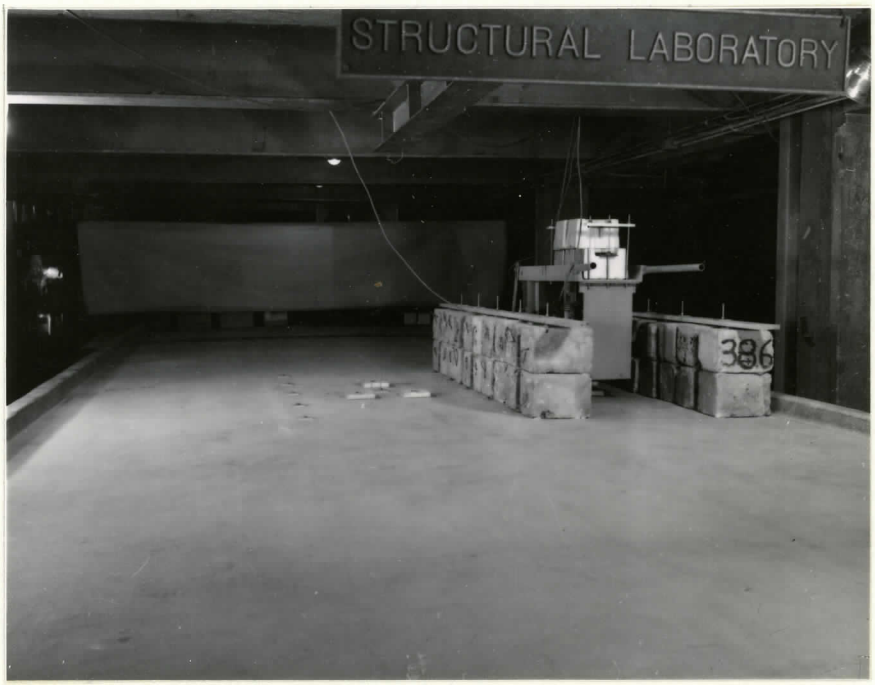
STRUCTURAL LABORATORY
386

RESULTS OF EXPERIMENTAL INVESTIGATION

Static Load Tests

The data obtained from the static load tests were reduced and calibration curves were plotted to obtain relationships such as load-strain, deflection-attenuator lines, and load-deflection. About 80 calibration curves were plotted. Except for beam A, or 1-1, with steel bearings, these curves showed a linear variation and the calibration constants were obtained from the slope of the curves. The data obtained for the exterior beam on the side farthest from the load--beam A for strain, or 1-1 for deflection--for steel bearings were too widely scattered to obtain reliable calibration constants. This was due, partly, to the small magnitudes involved.

A typical calibration curve is shown in Fig. 13, Appendix A. The values of the different calibration constants are tabulated in Table 3.

It appears from the values of the calibration constants that all beams of the model bridge deflect downward, when a downward load is applied eccentrically at midspan. In this investigation, the load was applied at midspan between beams (C) and (D) (Fig. 2). From the values of the constant C_1 for different bearing conditions, it is seen that the deflection of the beams at midspan is in decreasing order of magnitude

TABLE 3

TYPICAL CALIBRATION CONSTANTS FROM STATIC LOAD TESTS

μ, micro-in./in.[a] = C_1(Δ, dial divisions)

Bearings	C_1 Beam 1-1	C_1 Beam 2-1	C_1 Beam 3-1	C_1 Beam 4-1
Curved steel sole plate	----	13.33	5.79	4.09
64 durom. pads	-66.00	12.50	5.00	3.30
49 durom. pads	-63.64	12.37	4.93	3.25

μ, micro-in./in.[a] = C_2(Δ, deflection attenuator lines, single amplitude[b])

Bearings	C_2 Beam 1-1	C_2 Beam 2-1	C_2 Beam 3-1	C_2 Beam 4-1
Curved steel sole plates	----	10.67	5.12	3.50
64 durom. pads	-61.00	10.50	4.50	2.96
49 durom. pads	-56.67	10.46	4.40	2.93

---

[a] unit strain reading for load cell. Load, P, lb = 4.95μ

[b] Oscillograph pen movement

TABLE 3--Continued

μ, micro-in./in.[a] = C_3(Δ, strain attenuator lines, single amplitude[b])

Bearings	C_3 Beam A	C_3 Beam B	C_3 Beam C	C_3 Beam D
Curved steel sole plates	---	19.60	6.35	4.88
64 durom. pads	-125.00	20.75	5.56	4.10
49 durom. pads	-133.33	21.27	5.63	4.20

Δ, deflection dial divisions = C_6(Δ, strain attenuator lines single amplitude[b])

$$C_6 = \frac{C_3}{C_1}$$

Bearings	C_6 Beam A	C_6 Beam B	C_6 Beam C	C_6 Beam D
Curved steel sole plates	----	1.47	1.10	1.19
64 durom. pads	1.89	1.66	1.11	1.24
49 durom. pads	2.10	1.72	1.14	1.29

TABLE 3--Continued

Δ, deflection dial divisions = C_7(Δ, deflection attenuator lines, single amplitude)

$$C_7 = \frac{C_2}{C_1}$$

Bearings	C_7 Beam 1-1	C_7 Beam 2-1	C_7 Beam 3-1	C_7 Beam 4-1
Curved steel sole plates	----	0.80	0.88	0.86
64 durom. pads	0.92	0.85	0.89	0.90
49 durom. pads	0.89	0.85	0.89	0.90

Δ, dial divisions = ES[c] (Δ , deflection attenuator lines)

Bearings	ES point 4-2	ES point 3-2	ES point 2-2	ES point 1-2
64 and 49 durom. pads	0.4440	0.4636	0.4458	0.4361

Δ, dial divisions = EN[d] (Δ , deflection attenuator lines)

Bearings	EN point 3-3	EN point 4-3	EN point 1-3	EN point 2-3
64 and 49 durom. pads	0.4435	0.4563	0.4368	0.4314

---

[c] south end of bridge

[d] north end of bridge

from (D) to (A). Also, the values of the calibration constants show that the total deflection at midspan--for a given load--is higher for neoprene than with steel supports. This is as expected since, in the case of neoprene, the supports also deflect, adding to the total deflection.

Based upon the reasoning that regardless of whether the supports are rigid or flexible--as in the case of neoprene--the net deflection of a beam is the same for a particular load, it would be expected that the strain in a particular beam would be the same for a given load regardless of the type of bearing conditions. However, the calibration constants show that a greater load is required to produce a particular strain with steel bearings than with neoprene pads. As explained by Emanuel (3), the friction between the curved steel sole plate and the bearing (masonry) plate and the shear modulus of the neoprene pads influence these static load deflections. The relationship for dynamic strains is not necessarily the same.

Natural Frequency

The data obtained from the oscillograph recordings of strain and deflections at midspan, for the different bearing conditions and free vibration, were reduced to obtain the natural frequencies of the bridge. Frequencies were first calculated from the oscillograph charts in terms of in./cycle and then converted to cycles/sec.

Experimental natural frequency values are shown in Table 4.

TABLE 4

EXPERIMENTAL NATURAL FREQUENCIES

	Supports	Frequency, cps			Number of values averaged
		Avg.	Max.	Min.	
Oscillator only	Steel	8.66	9.11	8.34	8
	64 durom.	7.62	7.87	7.29	20
	49 durom.	7.61	7.87	7.13	20
Oscillator with concrete blocks	Steel	7.69	8.20	7.29	12
	64 durom.	7.16	7.87	6.65	22
	49 durom.	6.66	6.93	6.43	8

Bridge Damping

In any theoretical solution of a bridge vibration problem, the damping characteristics of the structure are very important. Bridge damping is generally considered to be a combination of coulomb and viscous types. Determination of damping coefficients, on the basis of coulomb or frictional damping, from experimental data is laborious and involves several assumptions. However, it is simple and straightforward to calculate the damping coefficient on the basis of viscous damping, and this is the method usually used for bridge calculations.

Thus, logarithmic decrements were calculated from the oscillograph recordings on the basis of viscous damping. In general, the first two cycles of maximum readable oscillation were used.

The logarithmic decrement is given by the equation (17, p. 60)

$$\delta = \frac{1}{n} (\ln Q) \qquad (2)$$

where,

δ = logarithmic decrement

n = number of cycles

$Q = \frac{x_o}{x_n}$

x_o = amplitude of initial vibration

x_n = amplitude of nth vibration

The logarithmic decrement can also be expressed as

$$\delta = \frac{2\pi\xi}{\sqrt{1 - \xi^2}} \qquad (3)$$

where,

ξ = damping factor

If ξ is appreciably less than unity, the logarithmic decrement can be approximated as

$$\delta \doteq 2\pi\xi \qquad (4)$$

Experimental values for logarithmic decrements and average damping factors are shown in Table 5. These values have been calculated on the basis of small amplitudes and viscous

damping, and the average damping factor is very small. Damping may become more significant in the case of forced vibrations near resonance or perhaps under impact loading.

TABLE 5

LOGARITHMIC DECREMENTS AND AVERAGE DAMPING FACTORS

	Supports	Logarithmic decrement			Number of values averaged	Average damping factor
		Avg.	Max.	Min.		
Oscillator only	Steel	0.151	0.166	0.122	8	0.0240
	64 durom.	0.147	0.184	0.122	22	0.0234
	49 durom.	0.144	0.163	0.124	20	0.0229
Oscillator with concrete blocks	Steel	0.153	0.205	0.122	12	0.0244
	64 durom.	0.151	0.179	0.115	22	0.0240
	49 durom.	0.149	0.182	0.131	8	0.0237

Vibration Tests

Data for strain and deflection were reduced from the oscillograph chart recordings. Strain data were reduced for values of frequency, dynamic strain in the bottom flange of each girder at midspan, applied driving force and strain amplification factor.

Deflection data for steel bearings were reduced for values of frequency, deflection at midspan of girders, forcing functions and deflection amplification factor.

Deflection data for neoprene pads were reduced for

values of frequency, gross deflection at the midspan and ends of the girders, forcing function, and gross deflection amplification factors at midspan. Representative values for strain and deflection are given in Tables 6 and 7.

Graphs of various combinations of variables were plotted and composite graphs were drawn. Typical plots are shown in Figs. 14-17, Appendix A.

Strain

Strain in the bottom flange of each girder is expressed in terms of inch per inch. Typical strain-frequency curves are shown in Figs. 18-25, Appendix A.

The following observations may be made from the data in Table 6 and the strain-frequency curves:

1. In general, although not always, the maximum strain, and hence the stress, in each girder at the respective natural frequency for each bearing condition was greater for curved steel sole plates than for neoprene pads.

2. For a given bearing condition the maximum dynamic strain at midspan of the girders is in an increasing order of magnitude from the unloaded to the loaded side.

3. The shape of strain-frequency curves for each bearing condition are essentially similar but displaced to the left for the elastomeric pads.

4. For any bearing condition the maximum dynamic strain in the girders was less when the bridge loaded with both

TABLE 6

MAXIMUM REDUCED VALUES FROM STRAIN DATA

	Supports	STA[a]	STB	STC	STD	AFSTA[b]	AFSTB	AFSTC	AFSTD
Vibrator only	Steel	100.5	126.0	155.0	190.0	---[c]	73.08	29.36	26.34
	64 durom.	70.5	92.5	139.0	179.0	271.35	58.73	33.30	23.08
	49 durom.	69.0	99.3	147.0	191.0	295.86	67.90	26.59	25.80
Vibrator with concrete blocks	Steel	38.0	80.0	125.0	178.0	---[c]	59.31	30.72	32.85
	64 durom.	24.0	55.0	118.0	169.0	82.22	51.51	28.84	30.51
	49 durom.	35.5	51.5	105.0	162.5	93.85	47.89	26.99	31.19

[a] strain (micro-in./in.), girder A

[b] Amplification factor (ϵ/ϵ_0) for strain, girder A

[c] No reliable values for amplification factor for girder (A) with steel supports could be obtained.

TABLE 7

MAXIMUM REDUCED VALUES FROM DEFLECTION DATA

	Supports	Y1-1[a]	Y2-1	Y3-1	Y4-1	AFY1-1[a]	AFY2-1	AFY3-1	AFY4-1
Vibrator only	Steel	----[b]	152.00	200.00	239.68		58.55	34.20	28.13
	64 durom.	97.02				196.17			
	49 durom.	95.68				192.50			
	64 durom.		139.02				55.90		
	49 durom.		144.66				59.80		
	64 durom.			199.50				36.19	
	49 durom.			198.81				33.17	
	64 durom.				257.73				30.38
	49 durom.				270.60				29.40
Vibrator with concrete blocks	Steel	----[b]	93.60	171.94	211.86		50.03	38.53	34.71
	64 durom.	31.42				52.14			
	49 durom.	43.39				54.48			
	64 durom.		79.17				42.90		
	49 durom.		77.41				44.16		
	64 durom.			156.60				34.36	
	49 durom.			147.63				33.64	
	64 durom.				224.50				32.88
	49 durom.				216.48				33.41

[a] Y1-1 is total dynamic deflection--downward or upward--at midspan of girder 1-1; AFY1-1 is deflection amplification factor (Δ/Δ_o) for midspan of girder 1-1.

[b] No reliable values could be obtained.

TABLE 7--Continued

	Supports	YS[c]	YN[c]	YEA[c]	YMN[c]	EPCYM[c]
Vibrator only	Steel					
	64 durom.	1.55	2.49	2.02	95.00	2.08
	49 durom.	4.86	5.82	5.34	90.34	5.58
	64 durom.	4.32	4.90	4.61	134.41	3.32
	49 durom.	7.42	7.30	7.36	137.30	5.09
	64 durom.	5.62	7.19	6.41	196.09	3.17
	49 durom.	9.72	10.90	10.31	189.50	5.16
	64 durom.	6.98	10.71	8.85	248.88	3.43
	49 durom.	11.34	14.08	12.72	257.88	4.70
Vibrator with concrete blocks	Steel					
	64 durom.	0.22	0.67	0.45	30.97	0.86
	49 durom.	1.33	2.02	1.58	41.81	2.90
	64 durom.	1.60	2.40	2.00	77.17	2.60
	49 durom.	3.36	3.19	3.28	74.13	4.24
	64 durom.	3.61	4.53	4.07	152.53	2.60
	49 durom.	6.02	6.93	6.48	141.15	4.39
	64 durom.	3.50	4.50	4.00	220.50	1.78
	49 durom.	8.61	9.50	9.06	207.42	4.19

[c]YS is end deflection at south end; YN is end deflection at north end; YEA is average end deflection; YMN is net deflection at midspan of girder; EPCYM is average end deflection expressed as per cent of gross midspan deflection. All deflections are in units of in.$(10)^{-3}$.

the oscillator and concrete blocks than when loaded with the oscillator only.

5. Differences in strain became negligible in the region of lower and higher frequencies.

Strain amplification factor

Strain amplification factor (ϵ/ϵ_o) is expressed as the ratio of dynamic strain to the strain which would be produced if the force was statically applied.

Typical strain amplification factor-frequency curves are given in Figs. 26-31, Appendix A. It may be noted from Table 6 and the curves that:

1. For girders (A) and (B) the values of strain amplification factors were considerably greater, when loaded with the oscillator only. For girders (C) and (D) the values were about the same for both loading conditions--oscillator only and oscillator plus concrete blocks.

2. In general, strain amplification factor values at midspan were in decreasing order of magnitude from the unloaded to loaded side.

3. The maximum strain amplification factor did not always occur at the maximum strain.

Deflection

Midspan deflection. Deflection at midspan of girders is expressed in inches. Typical deflection-frequency curves

are shown in Figs. 32-37, Appendix A.

From Table 7 and the curves the following deflection relationships may be seen:

1. Except for the exterior girder on the loaded side, the total, and thus the net, deflection at midspan was less for neoprene than for steel bearings, at the respective natural frequencies.

2. At the natural frequency, the maximum total midspan girder deflections were in increasing order of magnitude from unloaded to loaded side.

3. Maximum midspan deflection of girders were less when the bridge was loaded with both the oscillator and concrete blocks than for the oscillator only.

4. The deflection-frequency relationships are similar to the strain-frequency relationships for the three bearing conditions.

5. The shape of the deflection-frequency curves for different bearing conditions are essentially similar but displaced to the left for the elastomeric pads.

6. The curves show little difference in the magnitudes of deflections for the different bearing conditions at lower and higher frequencies.

End deflection. End deflections observed for the neoprene pads were of negligibly small amount. In general, the maximum average end deflections in the region of the natural

frequency, where they were most pronounced, were well below 5% of the total dynamic deflection at midspan. Also the supports at the north end, in general, deflected more than the supports at the south end.

Deflection amplification factor

Midspan deflection. Deflection amplification factor (Δ/Δ_o), a dimensionless factor, is expressed as the ratio of dynamic deflection to the deflection which would be produced if the force were statically applied. Typical deflection-amplification factor-frequency curves are shown in Figs. 38-43, Appendix A.

It may be observed from Table 7 and the curves that:

1. Except for girder (A), when the bridge is loaded with the oscillator only, the values of deflection-amplification factors, for the bridge with oscillator only and with oscillator and concrete blocks, are quite close for all three bearing conditions.

2. Values are in decreasing order of magnitude for girders from the unloaded to loaded side.

3. The curves show the same general relationships as those for strain.

THEORETICAL INVESTIGATION

A complete mathematical analysis of the dynamic behavior of the test bridge is beyond the scope of this study. This is partly due to the large number of variables involved and their complex nature and influence. These include the cracks in the deck slab, number and arrangement of girders, type and degree of damping, and the difficulty in expressing boundary conditions, torsional rigidity, mass moment of inertia, etc. Therefore, simplifying assumptions will be made for calculation of the natural frequencies and amplitude of dynamic deflections.

Natural Frequency

For calculation of natural frequency it is often assumed that the bridge behaves as a simply supported single beam. One method for determination of the natural frequency of a beam on elastic supports which takes into account the applied load and also the two equivalent masses of the supports is given by Jacobsen and Ayre (7, p. 86). Using the static deflection approach, they obtain

$$p^2 = g \frac{Wi \Delta i}{Wi \Delta i^2} \qquad (5)$$

where,

p = natural frequency of the system, rad/sec

g = acceleration due to gravity, in./sec^2

Wi = weight of the mass of individual concentrated loads, equivalent mass of the beam, and equivalent mass of supports, lb

Δi = deflection of respective Wi weights, in.

An empirical formula suggested for determining the weight, wleq, of the equivalent mass of the beam is:

$$wleq = \left[\frac{17}{35} + \frac{18}{35} \tanh \frac{\delta av}{\delta o} \right] wl \qquad (6)$$

where,

δav = midspan deflection due to supports, in.

δo = midspan deflection due to dead load of beam plus concentrated loads, in.

An equivalent beam on rigid supports is shown in Fig. 7.

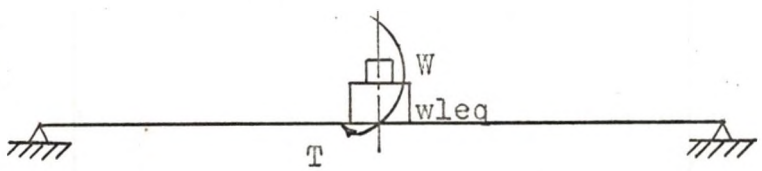

Fig. 7. Beam on rigid supports

Modifying the above formula to take torsion into account gives

$$p^2 = \frac{\sum Wi\ \Delta i + T\theta}{\sum \frac{Wi}{g}\ \Delta i^2 + J\theta^2} \qquad (7)$$

For this case,

wleq = weight of the equivalent mass of the beam; 5356 lb

W = weight of oscillator; 644 lb

T = Torque; 2100 ft-lb

An equivalent beam on elastic supports is shown in Fig. 8.

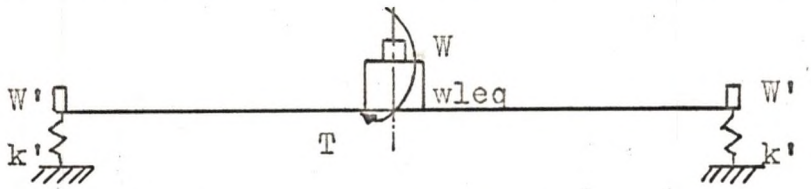

Fig. 8. Beam on elastomeric supports

k' = stiffness of neoprene pads; 259,200 lb/in. for the 64 durom. pads and 140,000 lb/in. for the 49 durom. pads.

W' = weight of support mass; negligible in this case.

The experimental and theoretical natural frequencies for the test bridge with oscillator (only) are shown in Table 8 for comparison.

TABLE 8

COMPARATIVE NATURAL FREQUENCIES

Type of support	Experimental cycles/sec	Theoretical cycles/sec
Steel	8.66	10.01
64 durom.	7.62	9.41
49 durom.	7.61	8.45

The experimental values show reasonable correlation with the analytical values. This is primarily due to the variables

previously listed. Also, analytical methods generally give values higher than those obtained experimentally, especially at the fundamental frequency.

Amplitude of Dynamic Deflection

For calculation of the deflection at midspan, neglecting torsion, the bridge and its equivalent system for rigid support condition is shown in Fig. 9.

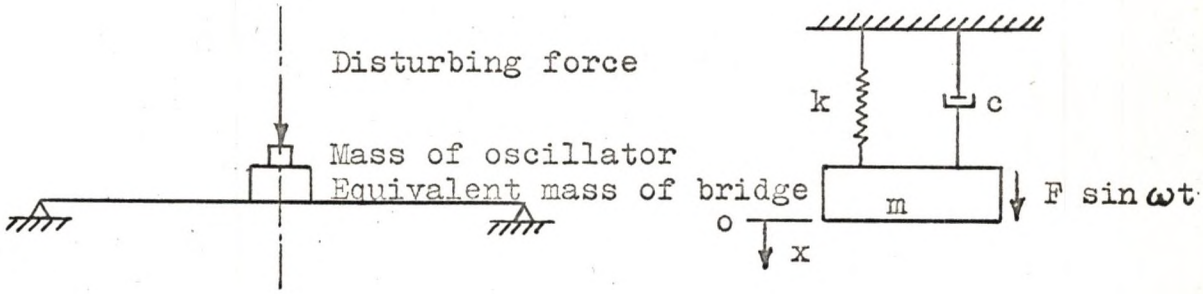

Fig. 9. The bridge on rigid supports and its equivalent system

For a particular frequency, ω, the equation of motion is (17, p. 51)

$$m\ddot{x} + c\dot{x} + kx = F \sin \omega t \qquad (8)$$

where,

m = mass, lb-sec^2-in.

c = coefficient of damping, lb-sec/in.

k = spring constant, lb/in.

F sin ωt = forcing function

The solution of the above equation, considering the steady-state response only, is

$$xp = X \sin (\omega t - \phi) \qquad (9)$$

where,

ϕ = phase angle

X = amplitude of dynamic deflection, in.

$$= \frac{F}{k\sqrt{(1-r^2)^2 + 4\varsigma^2 r^2}}$$

where,

k = spring constant, lb/in.

ς = damping factor, dimensionless

$r = \frac{\omega}{\omega n}$, ωn being the natural frequency, rad/sec

For a beam on elastomeric supports the spring and damping action of the pads must be taken into account (Fig. 10).

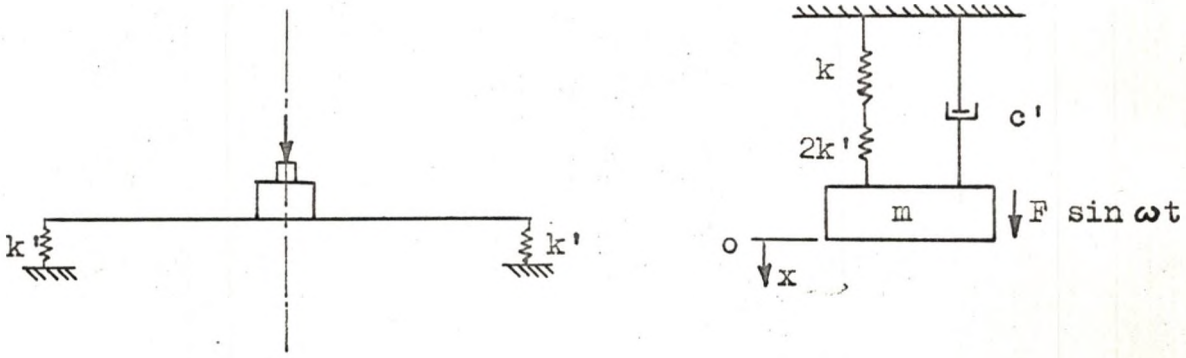

Fig. 10. The bridge on elastomeric supports and its equivalent system

The effective spring constant is:

$$ke = \frac{2\,k' \cdot k}{2\,k' + k} \qquad (10)$$

Comparative theoretical and experimental dynamic deflections of the test bridge, at the center line of midspan, with

oscillator (only) are shown in Table 9.

TABLE 9

COMPARATIVE THEORETICAL AND EXPERIMENTAL DYNAMIC DEFLECTION AT MIDSPAN, NEGLECTING TORSION

Type of support	Frequency cycles/sec	Deflection	
		Experimental in.	Theoretical in.
Steel	8.51	0.176	0.086
64 durom.	7.53	0.165	0.109
49 durom.	7.51	0.172	0.102

Consideration of the torsional movement of the bridge makes the problem more complicated. It is assumed that a cross-section of the bridge oscillates torsionally about the center of gravity (Fig. 11).

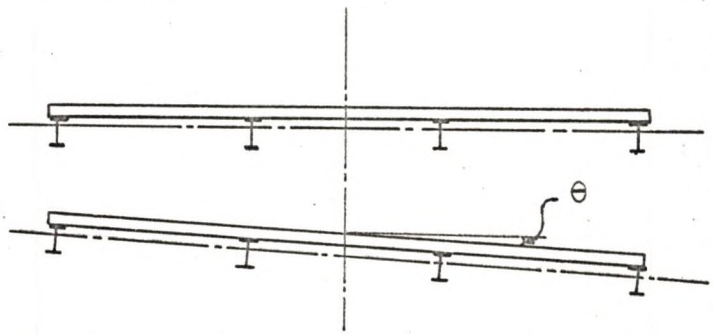

Fig. 11. Cross section of the bridge showing torsional distortion

The total dynamic deflection of any girder at a particular frequency will be the algebraic sum of the deflection at

the centerline of midspan, as previously discussed, and the deflection produced by torsional rotation of the cross-section. An equivalent system for torsion is shown in Fig. 12.

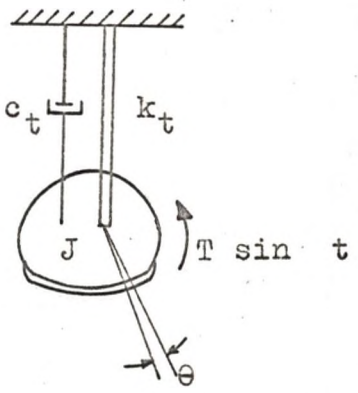

Fig. 12. Equivalent system of the bridge for torsion

The equation of motion for torsion can be written as (17, p. 51):

$$J\ddot{\theta} + C_t\dot{\theta} + k_t\theta = T \sin \omega t \qquad (11)$$

Considering steady state response only,

$$\theta p = \Theta \sin (\omega t - \phi) \qquad (12)$$

where,

ϕ = phase angle

Θ = amplitude of rotation

$$= \frac{T}{k_t \sqrt{(1-r^2)^2 + 4\xi^2 r^2}}$$

where,

k_t = spring constant, in.-lb/rad

Values for the torsional rigidity of the beam were calculated from the data obtained from static load tests. Damping factors were experimentally determined.

Comparative theoretical and experimental dynamic deflections for beams 3-1 and 4-1 with oscillator (only) are shown in Table 10.

TABLE 10

COMPARATIVE THEORETICAL AND EXPERIMENTAL DYANMIC DEFLECTION AT MIDSPAN, CONSIDERING TORSION

Type of support	Frequency cycles/sec.	Deflection			
		Experimental (in.)		Theoretical (in.)	
		Beam 3-1	Beam 4-1	Beam 3-1	Beam 4-1
Steel	8.51	0.200	0.240	0.148	0.242
64 durom.	7.53	0.200	0.258	0.174	0.305
49 durom.	7.51	0.199	0.269	0.163	0.285

It should be noted that theoretical values of dynamic amplitudes have been investigated under the assumption that a particular frequency remains steady. However, during the experimental investigation frequencies were varied from slow to fast and fast to slow. Besides, as stated before, near the natural frequency any attempt to increase or decrease the speed only increases the amplitude of dynamic deflection, which is probably due to the nonlinear spring characteristics

of the bridge. These are the main reasons for the difference between experimental and analytical values. Also, the assumed value for n, and ultimately EI, and the assumed value for k_t are, of necessity, approximate.

CONCLUSIONS

One model bridge, with a length of 25 ft and a roadway width of 10 ft was used in this investigation. It is recognized that the results obtained may differ widely from tests utilizing different test bridges, methods of forced vibration, or neoprene pads.

Therefore, the following conclusions should be considered indicative rather than conclusive, for the dynamic behavior of a model bridge on rigid and elastomeric bearings when a forced vibration is eccentrically applied.

1. For a given load, applied statically, the total deflection at midspan is higher for neoprene than with steel supports.
2. Neoprene bearing pads add to the damping of the bridge. The natural frequency of the bridge superstructure is higher with steel supports than with elastomeric bearings--the smallest spring modulus giving the lowest natural frequency.
3. In general, though not always, the maximum strain, and hence the stress, in each girder at the respective natural frequency for each bearing condition was greater for steel bearings than for neoprene. Also the total and the net deflection, under similar

conditions, were greater for steel except for the exterior girder on the loaded side.

4. For any bearing condition, the maximum dynamic strain (and hence the stress) and girder deflection are less when the bridge is loaded with both oscillator and concrete blocks than when loaded with the oscillator only. Thus, the dynamic stress and deflection--and also their amplification factors--of a loaded bridge are less than those of an unloaded one.
5. Amplification factors for strain and deflection for the exterior and interior girders on the loaded side are fairly close and are much less than the corresponding amplification factors of the other exterior and interior girders on the unloaded side.
6. At low and high frequencies (approximately 4 to 5½ and 9½ to 11½ cps for this investigation) the magnitudes of strain and deflection are quite close for different bearing conditions. At intermediate frequencies below the natural frequency the magnitudes of strain and deflection are greater for elastomeric than rigid bearings.
7. A torsional mode of vibration occurs when the dynamic load on the bridge is eccentrically applied. The torsional effect becomes more pronounced as the impressed frequency approaches the natural frequency in torsion.

REFERENCES CITED

1. Biggs, J. M. and Suer, H. S. Vibration measurements on simple span bridges. Highway Research Board Bulletin 124: 1-15. 1956.

2. Edgerton, R. C. and Beecroft, G. W. Dynamic studies of two continuous plate girder bridges. Highway Research Board Bulletin 124: 33-46. 1956.

3. Emanuel, J. H. Problems of bridge supporting and expansion devices and an experimental comparison of the dynamic behavior of rigid and elastomeric bearings. Unpublished Ph.D. thesis. Ames, Iowa, Library, Iowa State University of Science and Technology. 1965.

4. Foster, G. M. and Oehler, L. T. Vibration and deflection of rolled-beam and plate-girder bridges. Highway Research Board Bulletin 124: 79-110. 1956.

5. Hayes, J. M. and Sbarounis, J. A. Vibration study of three span continuous I-beam bridge. Highway Research Board Bulletin 124: 47-78. 1956.

6. Highway Research Board. Dynamic studies of bridges on the AASHO road test. Highway Research Board Special Report 71. 1962.

7. Jacobsen, L. S. and Ayre, R. S. Engineering vibrations. New York, N. Y., McGraw-Hill Book Co., Inc. 1958.

8. Ku, Y. H. Analysis and control of nonlinear systems. New York, N. Y., Ronald Press Co. 1958.

9. Linger, D. A. and Hulsbos, C. L. Dynamics of highway bridges. Iowa State Univ. of Sci. and Tech. Engr. Expt. Sta. Bulletin 188 and Iowa Highway Research Board Bulletin 17. 1960.

10. McCready, S. D. Elastomeric bridge bearings. Discussion on the paper by R. L. Pare and E. F. Keiner. Highway Research Board Bulletin 242: 18-19. 1960.

11. Myklestad, N. O. Fundamentals of vibration analysis. New York, N. Y., McGraw-Hill Book Co., Inc. 1956.

12. Ozell, A. M. and Diniz, J. F. Report on tests of neoprene pads under repeated shear loads. Highway Research Board Bulletin 242: 20-27. 1960.

13. Pare, R. L. and Keiner, E. P. Elastomeric bridge bearings. Highway Research Board Bulletin 242: 1-18. 1960.

14. Scheffey, C. F. Dynamic load analysis and design of highway bridges. Highway Research Board Bulletin 124: 16-32. 1956.

15. Senne, J. H. Distribution of loads in beam and slab floors. Unpublished Ph.D. thesis. Ames, Iowa, Library, Iowa State University of Science and Technology. 1961.

16. Senne, J. H. and Smith, T. K. Dynamics of highway bridges: Final Report, Project 376-S. Ames, Iowa, Iowa Engineering Experiment Station, Iowa State University of Science and Technology. 1961.

17. Tse, F. S., Morse, I. E., and Hinkle, R. T. Mechanical vibrations. 1st ed. Boston, Mass., Allyn and Bacon, Inc., 1964.

18. Tung, T. P., Goodman, L. E., Chen, T. Y., and Newmark, N. M. Highway bridge impact problems. Highway Research Board Bulletin 124: 111-134. 1956.

19. Wise, J. A. Dynamics of highway bridges. Highway Research Board Proceedings 32: 180-187. 1953.

20. Zuk, W. Bridge vibrations as influenced by elastomeric bearings. Highway Research Board Bulletin 315: 27-34. 1962.

APPENDIX A:

TYPICAL GRAPHS OF REDUCED DATA FROM EXPERIMENTAL INVESTIGATION

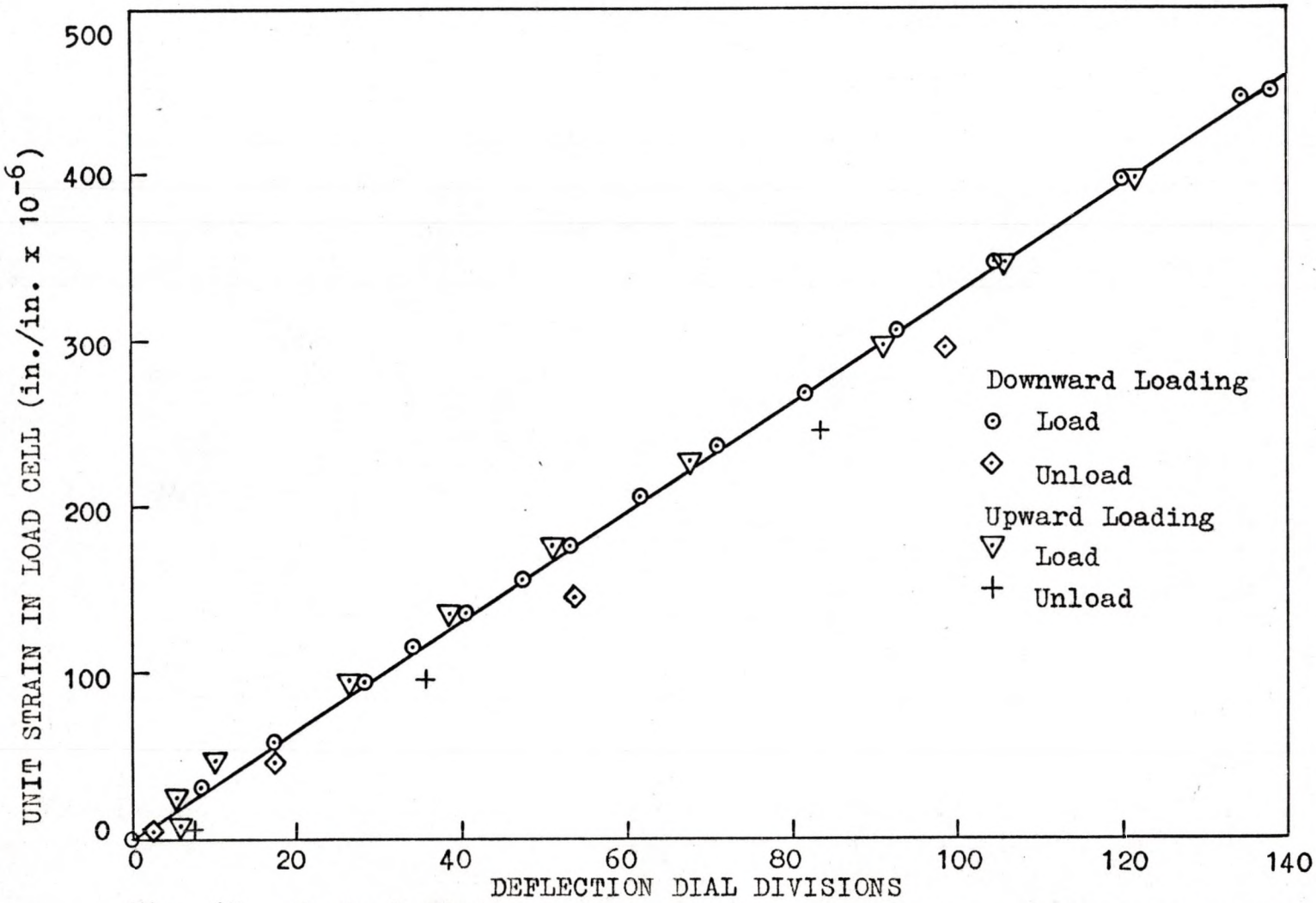

Fig. 13. Typical static load test calibration curve. Relationship between unit strain in load cell and deflection dial divisions, beam D, 49 durom.

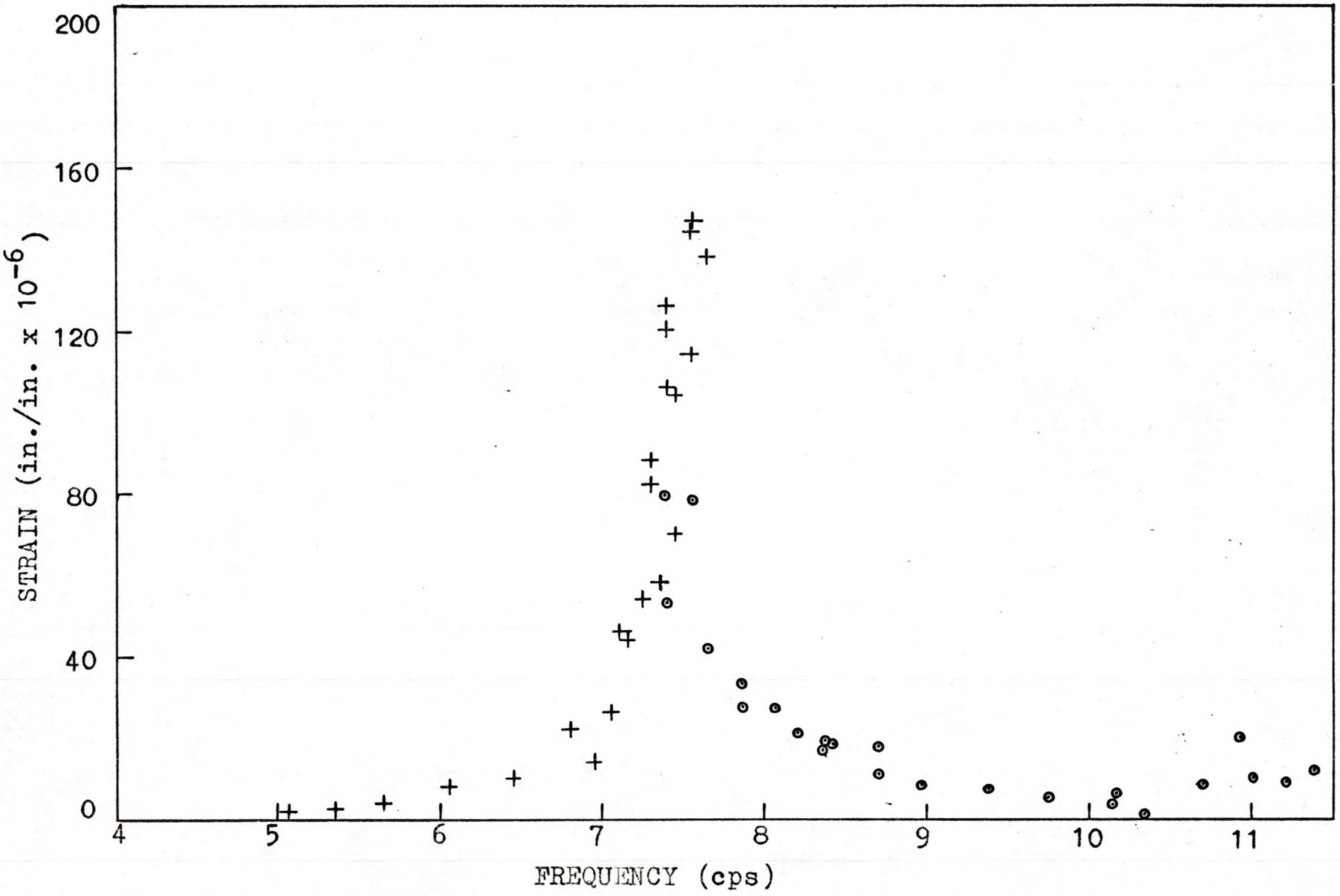

Fig. 14. Strain-frequency relationship for beam C, 49 durometer, oscillator only

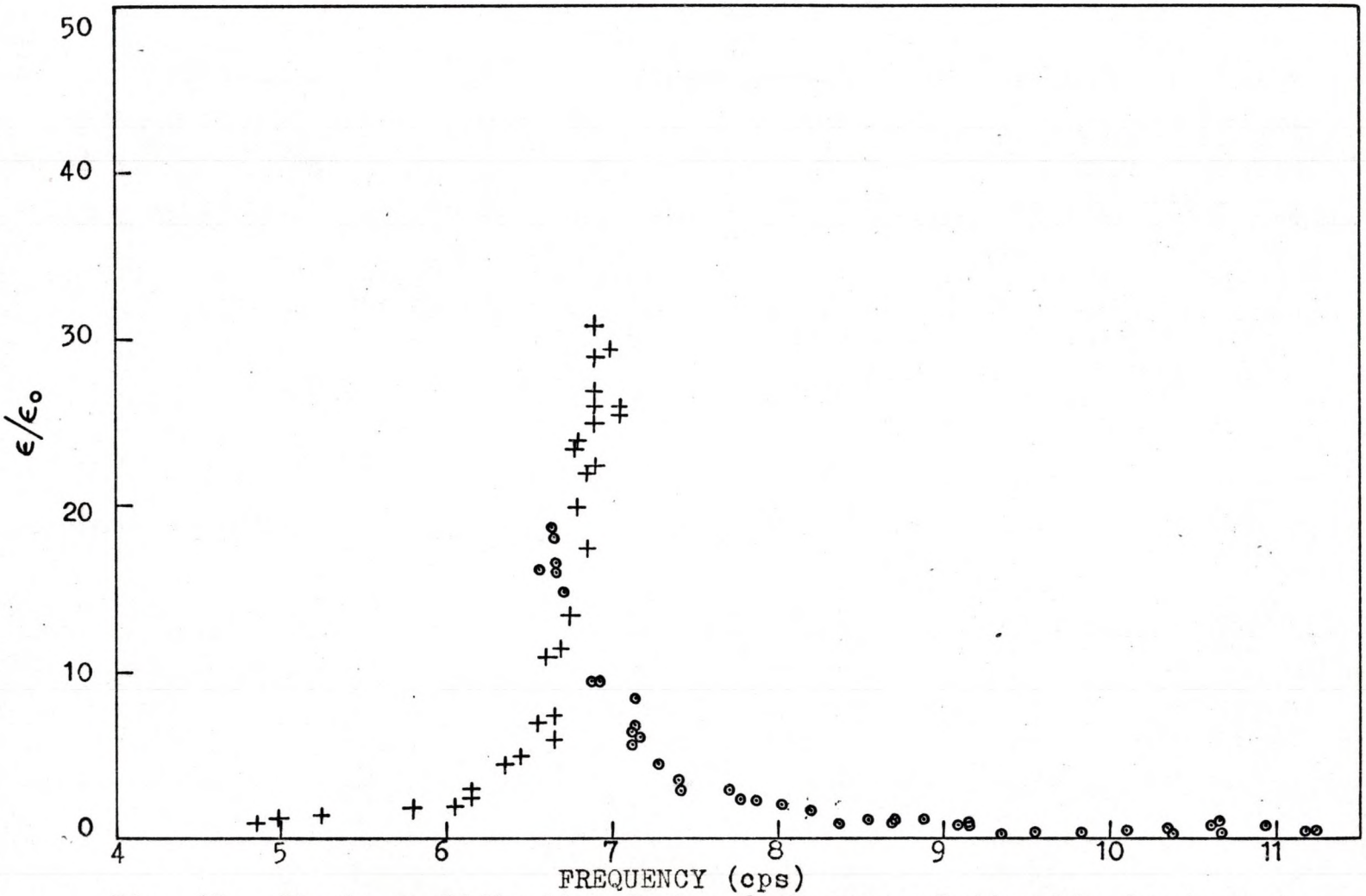

Fig. 15. Strain amplification factor-frequency relationship for beam C, curved steel sole plates, oscillator with concrete blocks

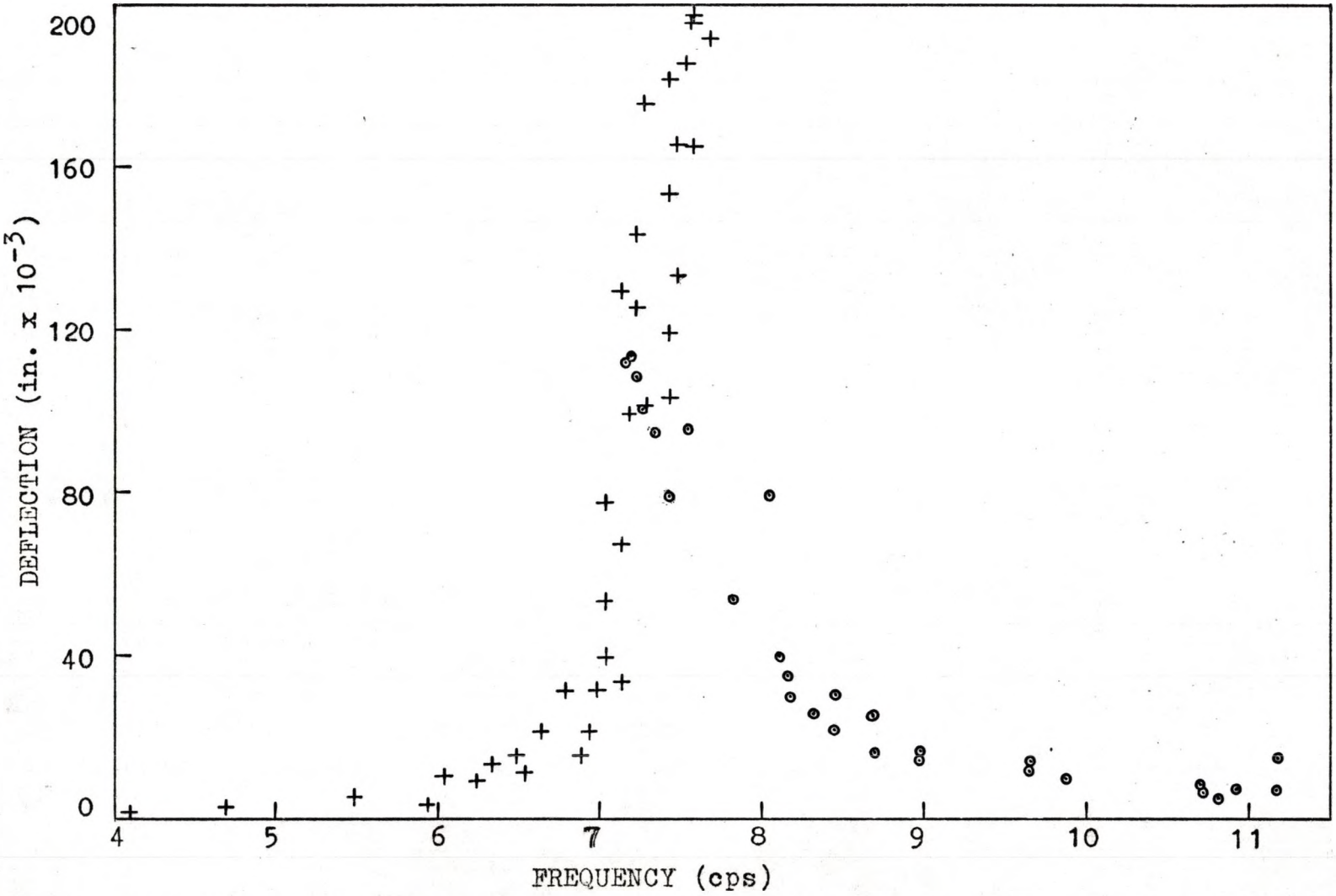

Fig. 16. Deflection-frequency relationship for beam 3-1, 64 durometer, oscillator only

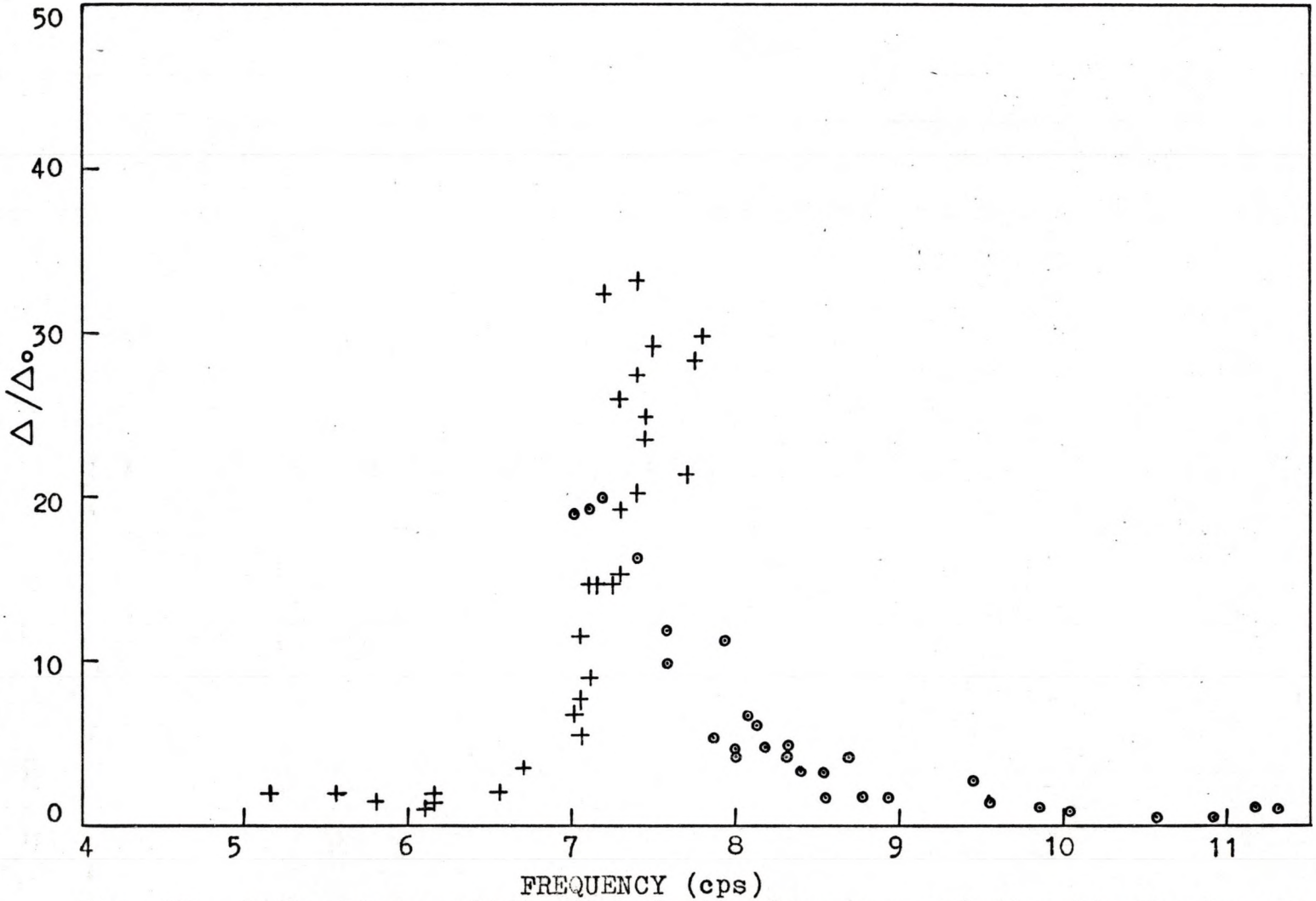

Fig. 17. Deflection amplification factor-frequency relationship for beam 3-1, 49 durometer, oscillator only

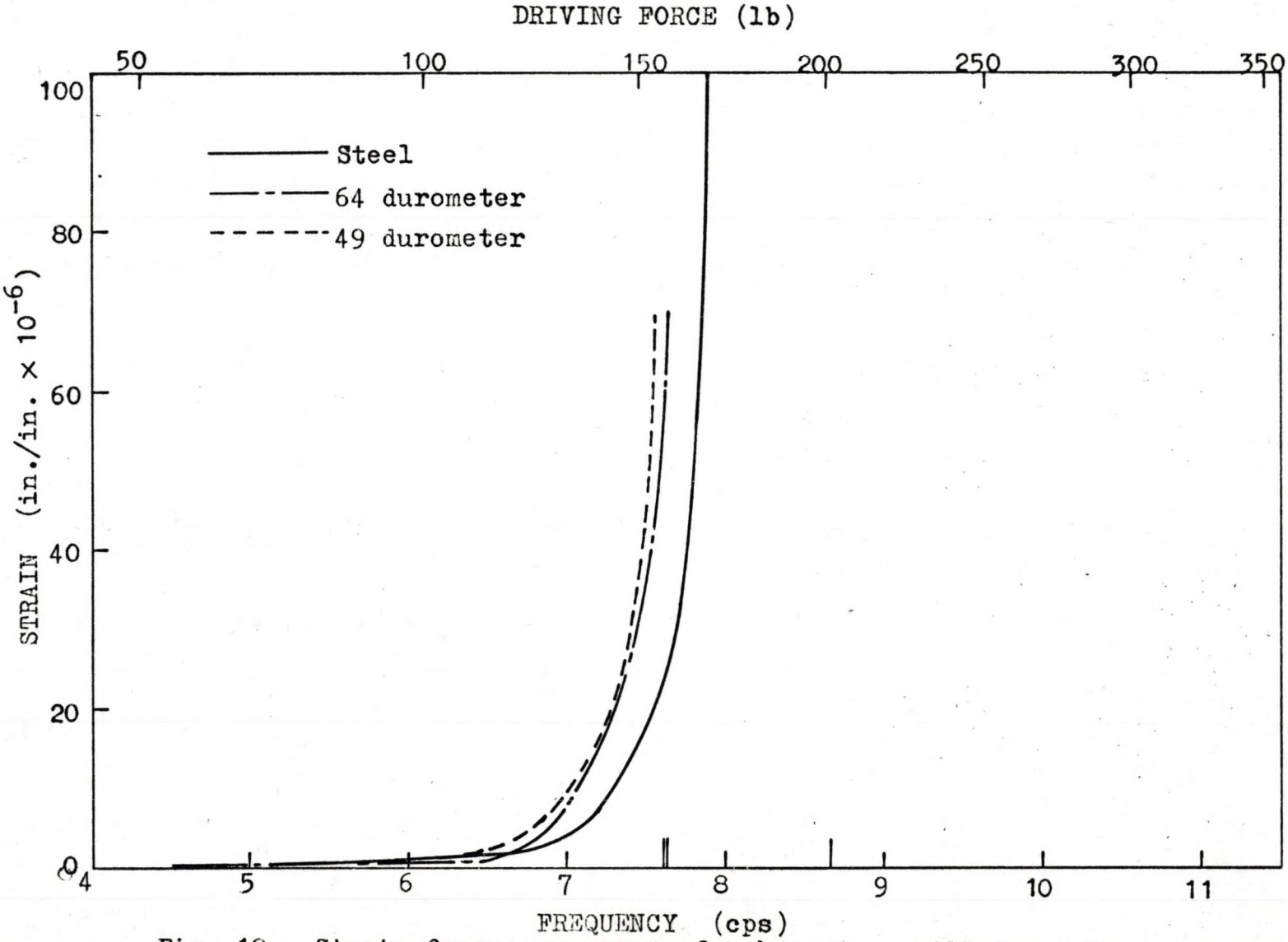

Fig. 18. Strain-frequency curves for beam A, oscillator only

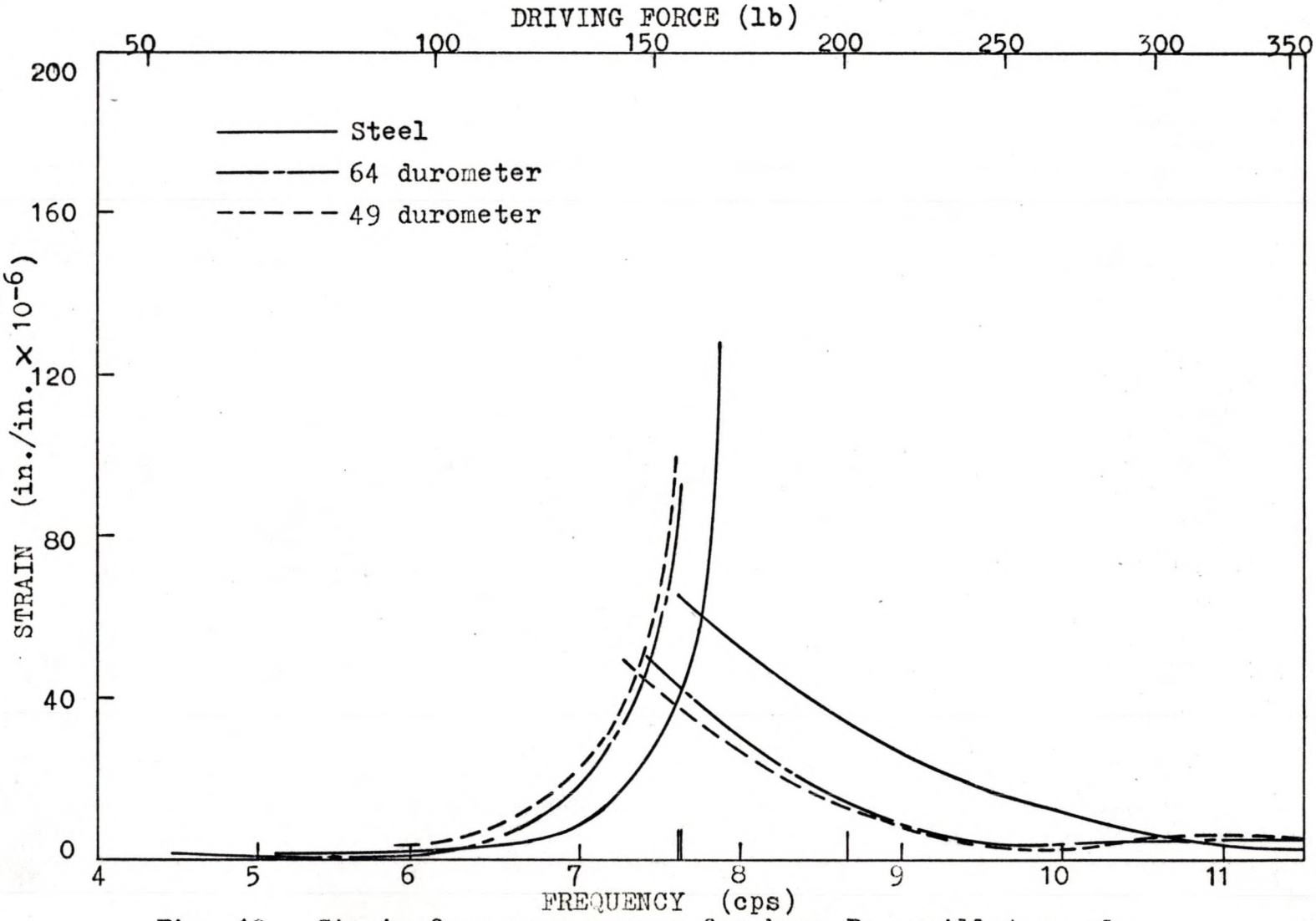

Fig. 19. Strain-frequency curves for beam B, oscillator only

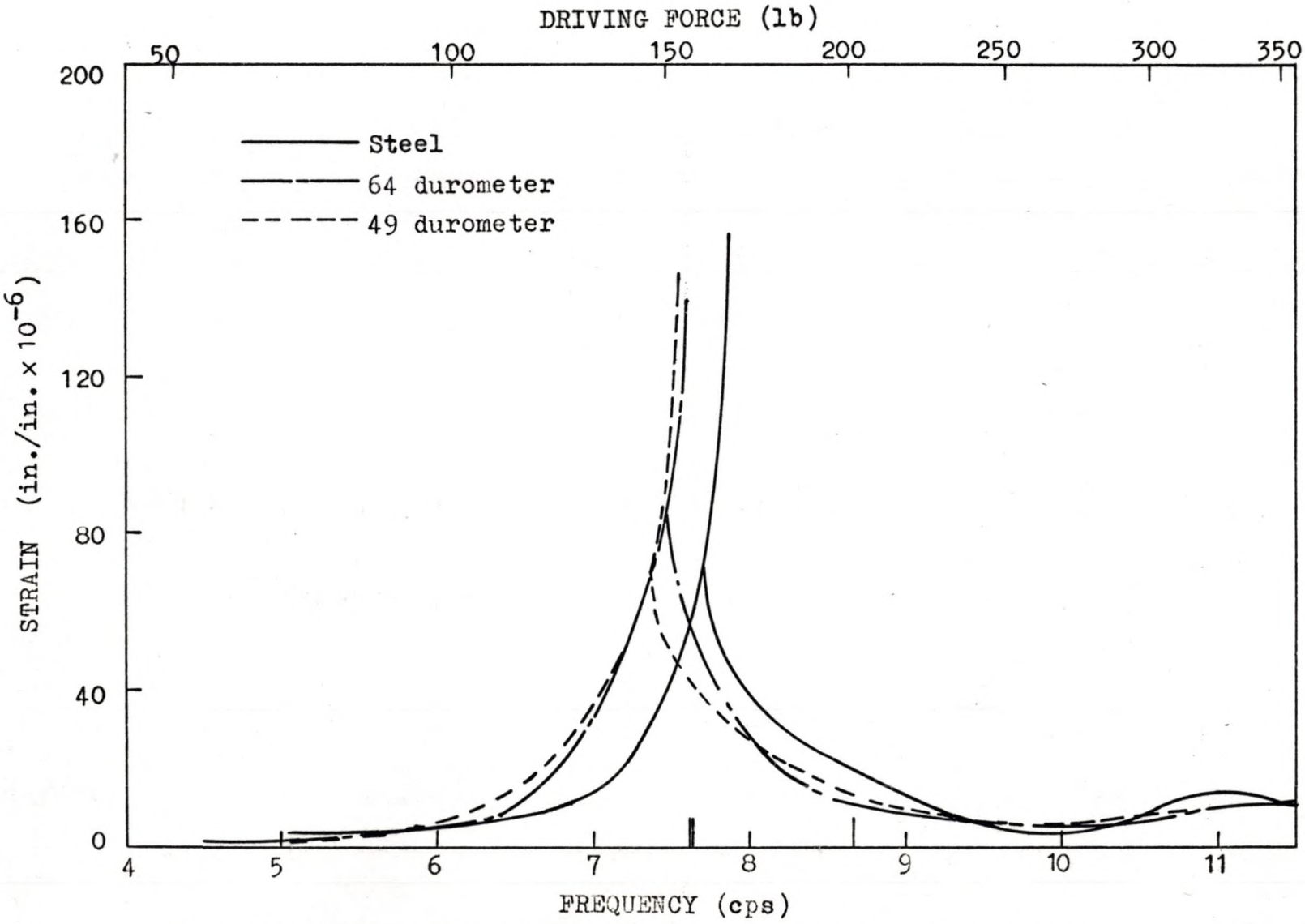

Fig. 20. Strain-frequency curves for beam C, oscillator only

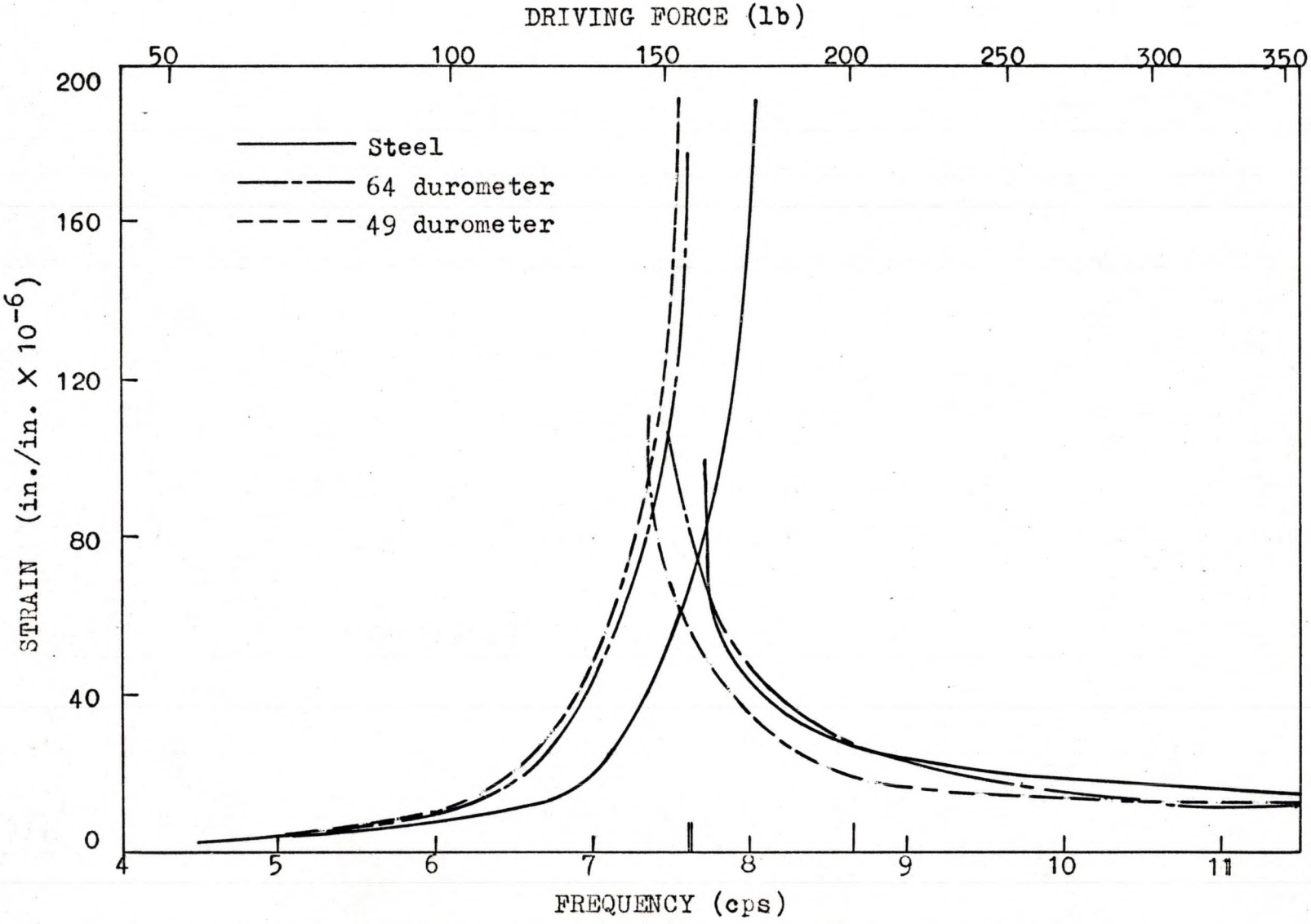

Fig. 21. Strain-frequency curves for beam D, oscillator only

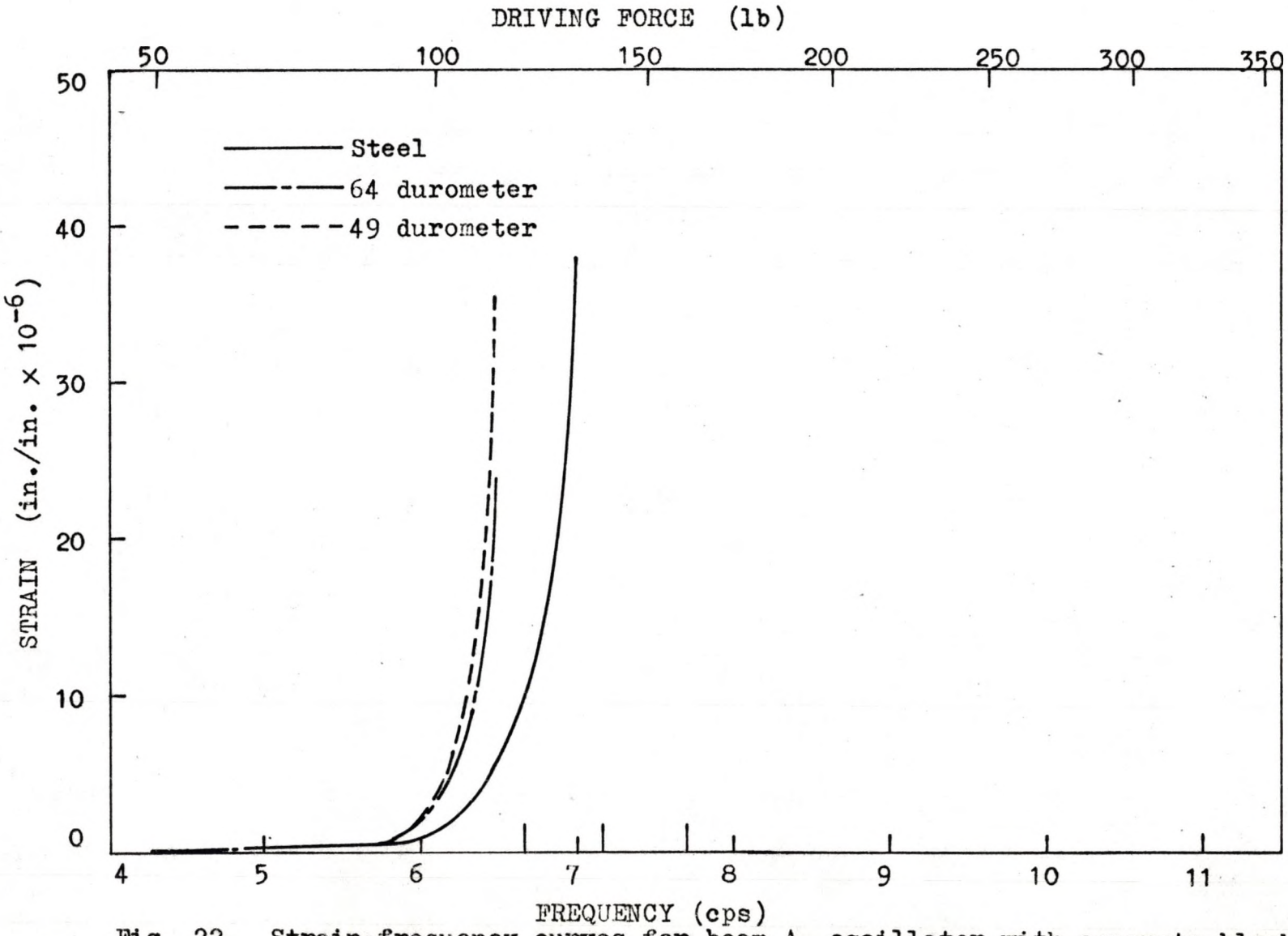

Fig. 22. Strain-frequency curves for beam A, oscillator with concrete blocks

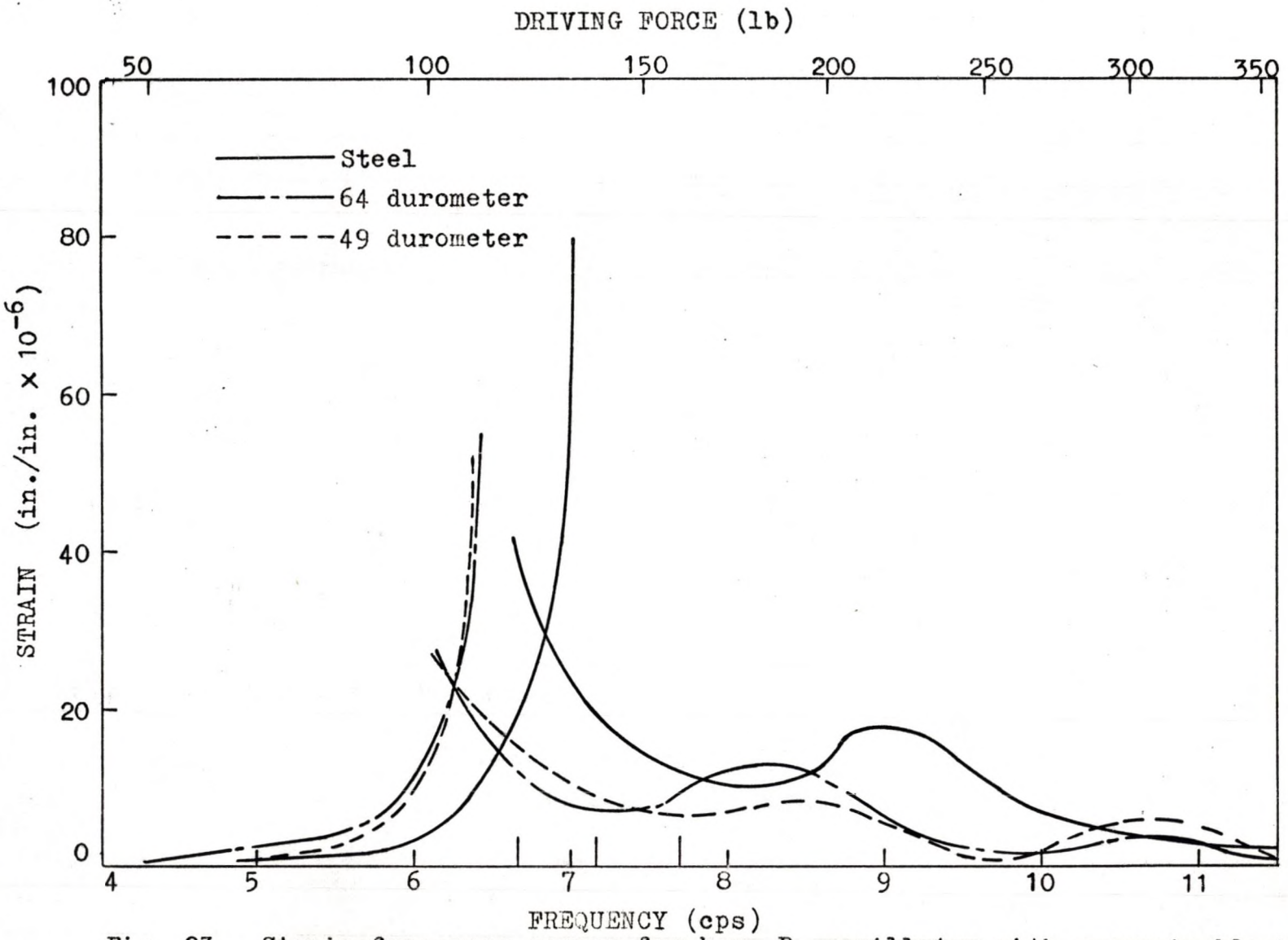

Fig. 23. Strain-frequency curves for beam B, oscillator with concrete blocks

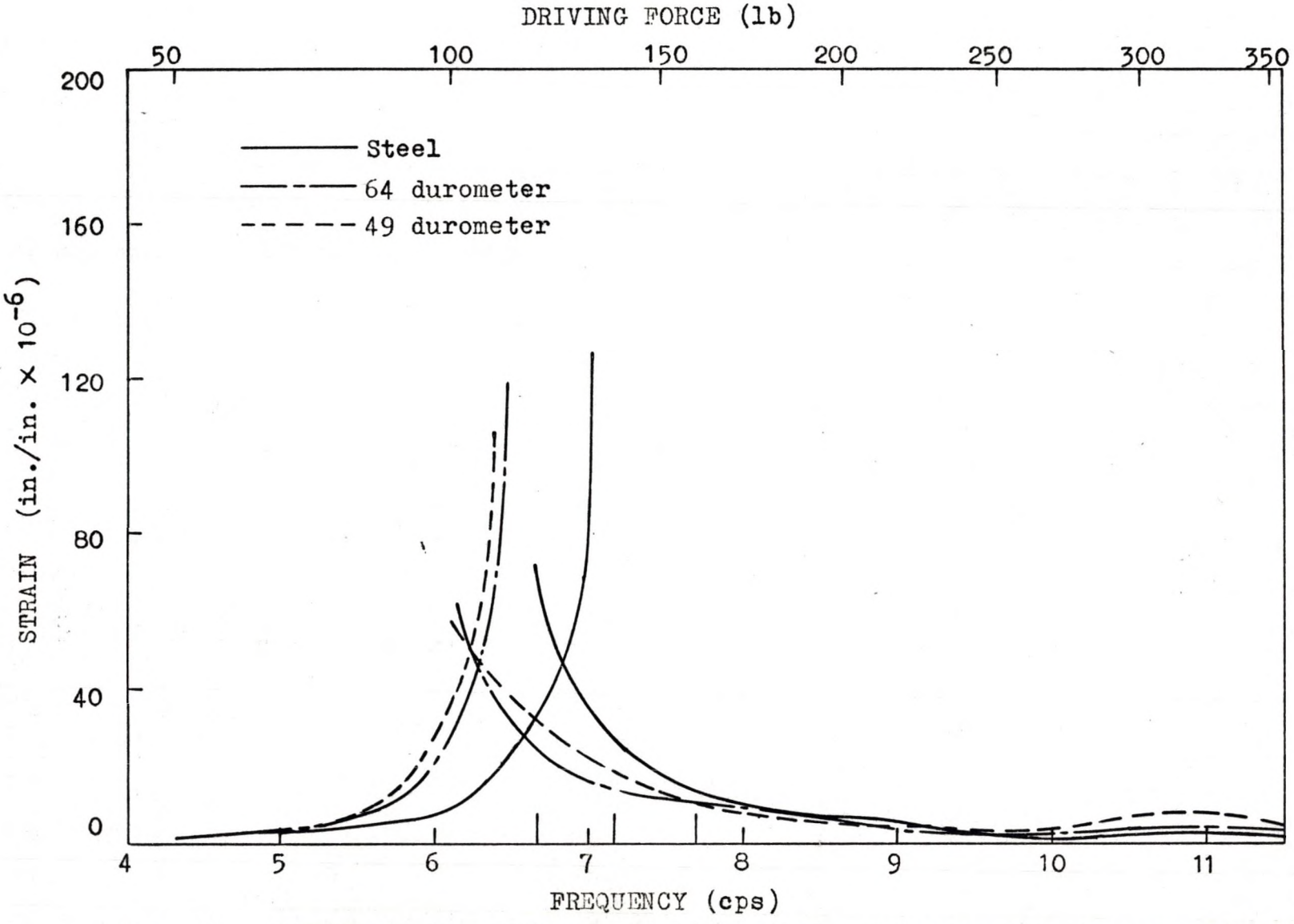

Fig. 24. Strain-frequency curves for beam C, oscillator with concrete blocks

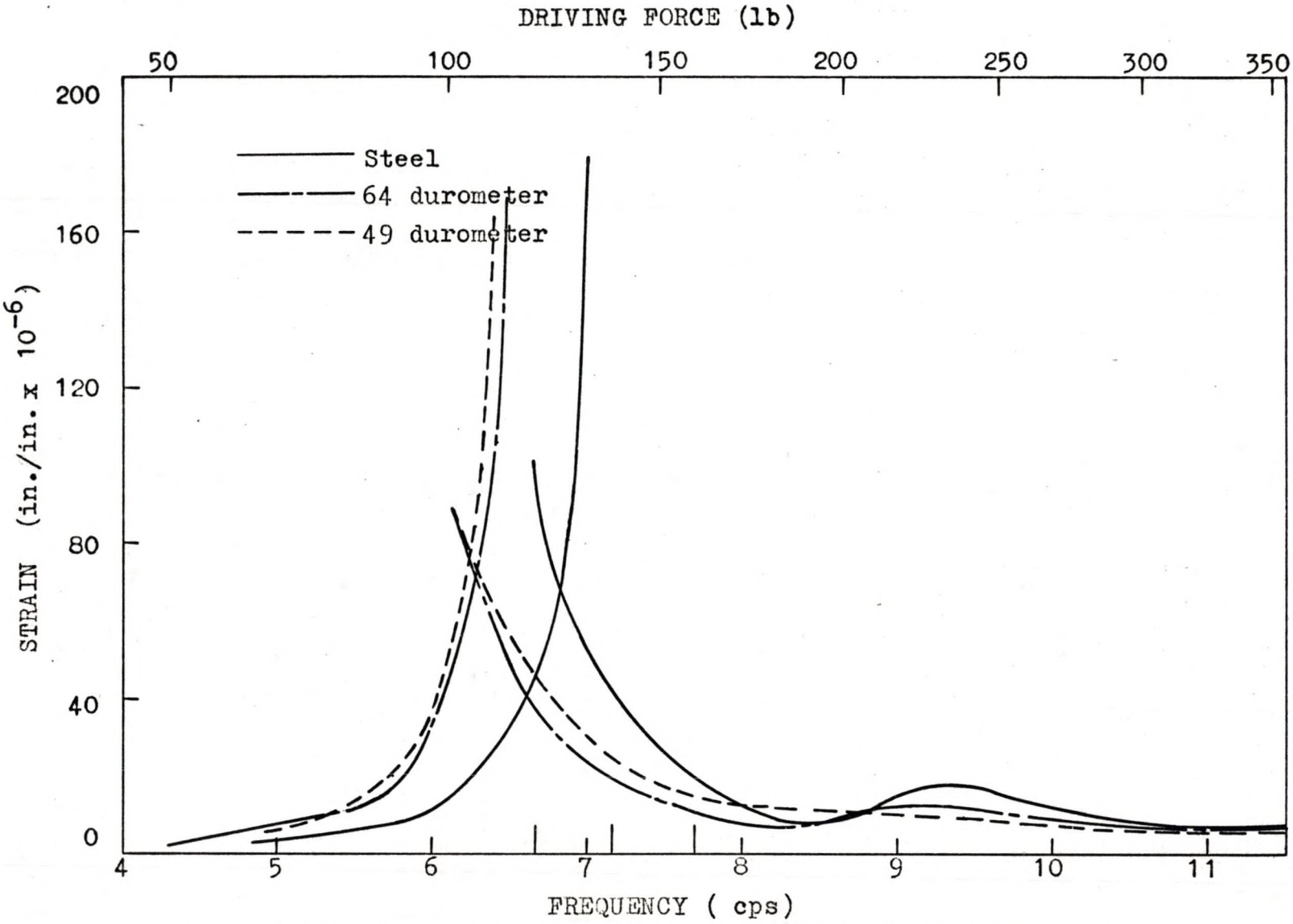

Fig. 25. Strain-frequency curves for beam D, oscillator with concrete blocks

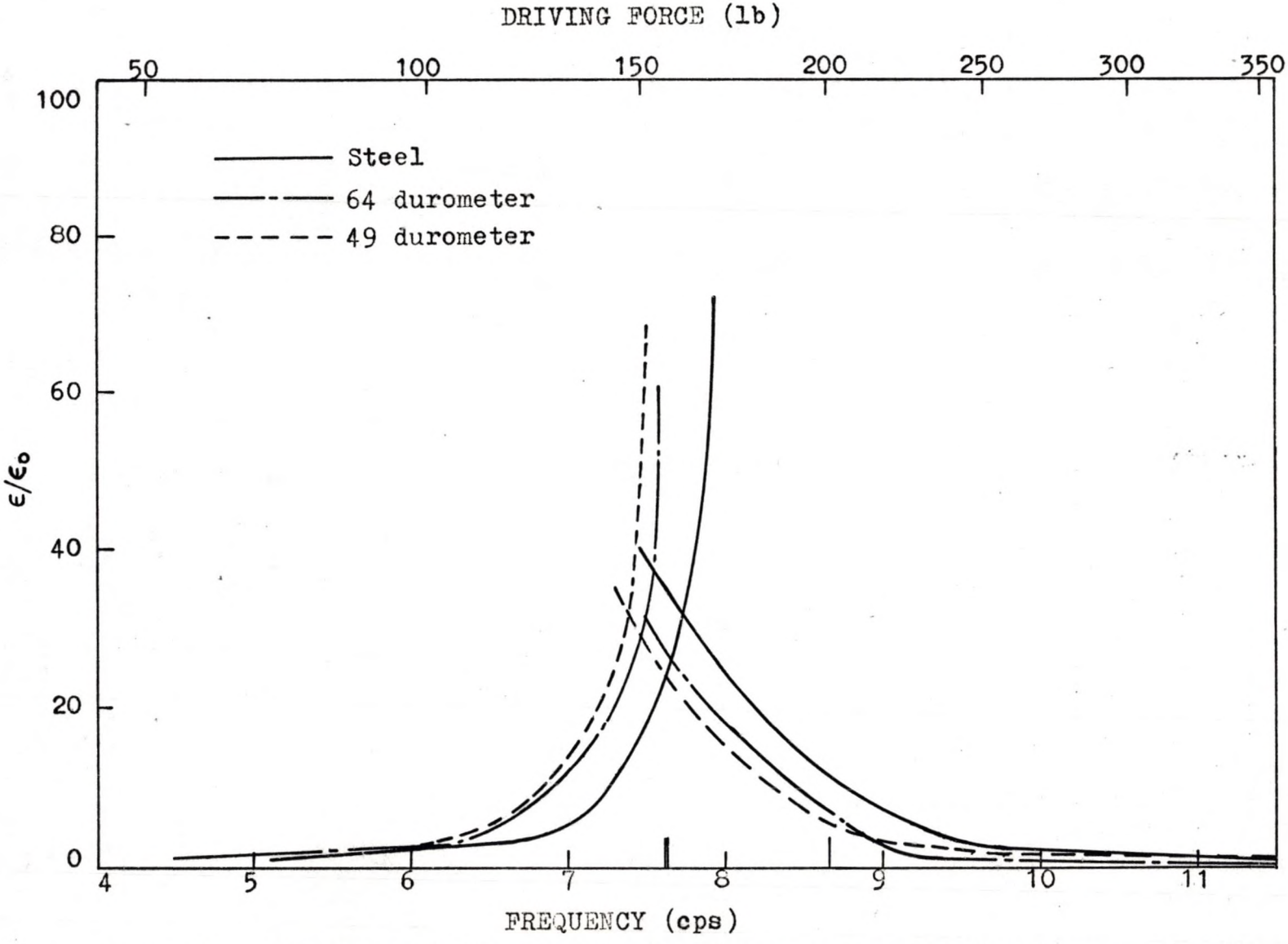

Fig. 26. Strain amplification factor-frequency curves for beam B, oscillator only

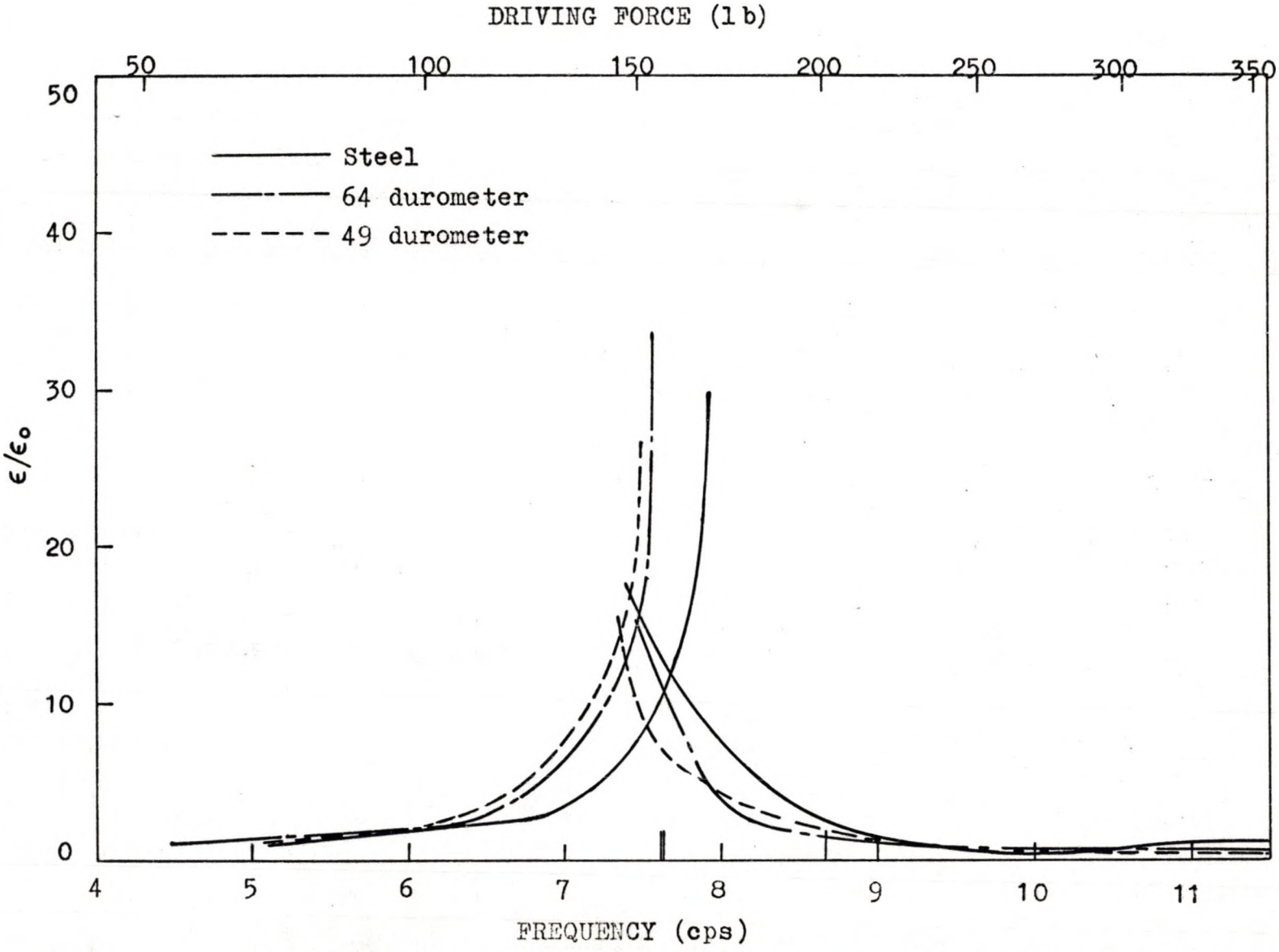

Fig. 27. Strain amplification factor-frequency curves for beam C, oscillator only

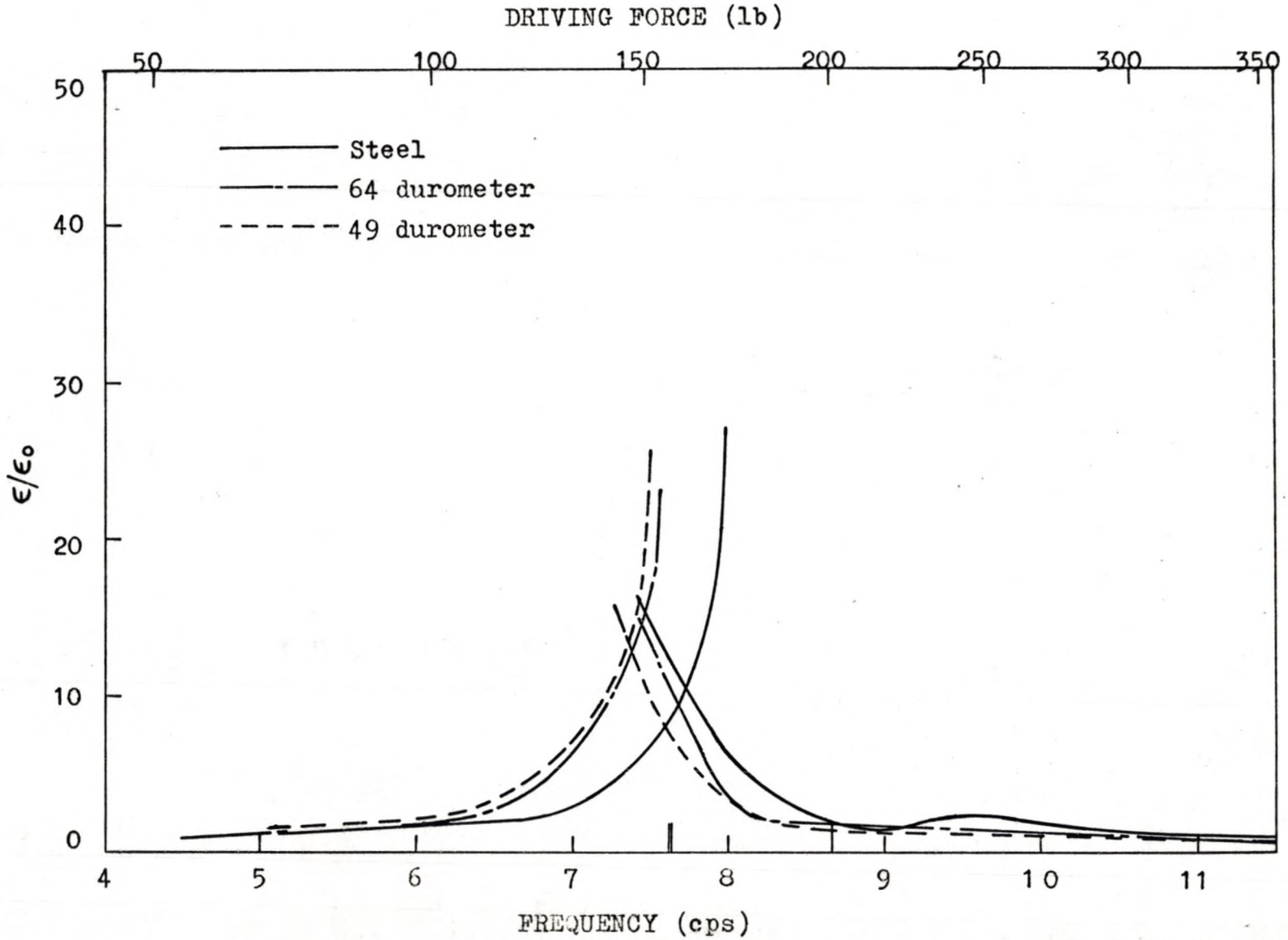

Fig. 28. Strain amplification factor-frequency curves for beam D, oscillator only

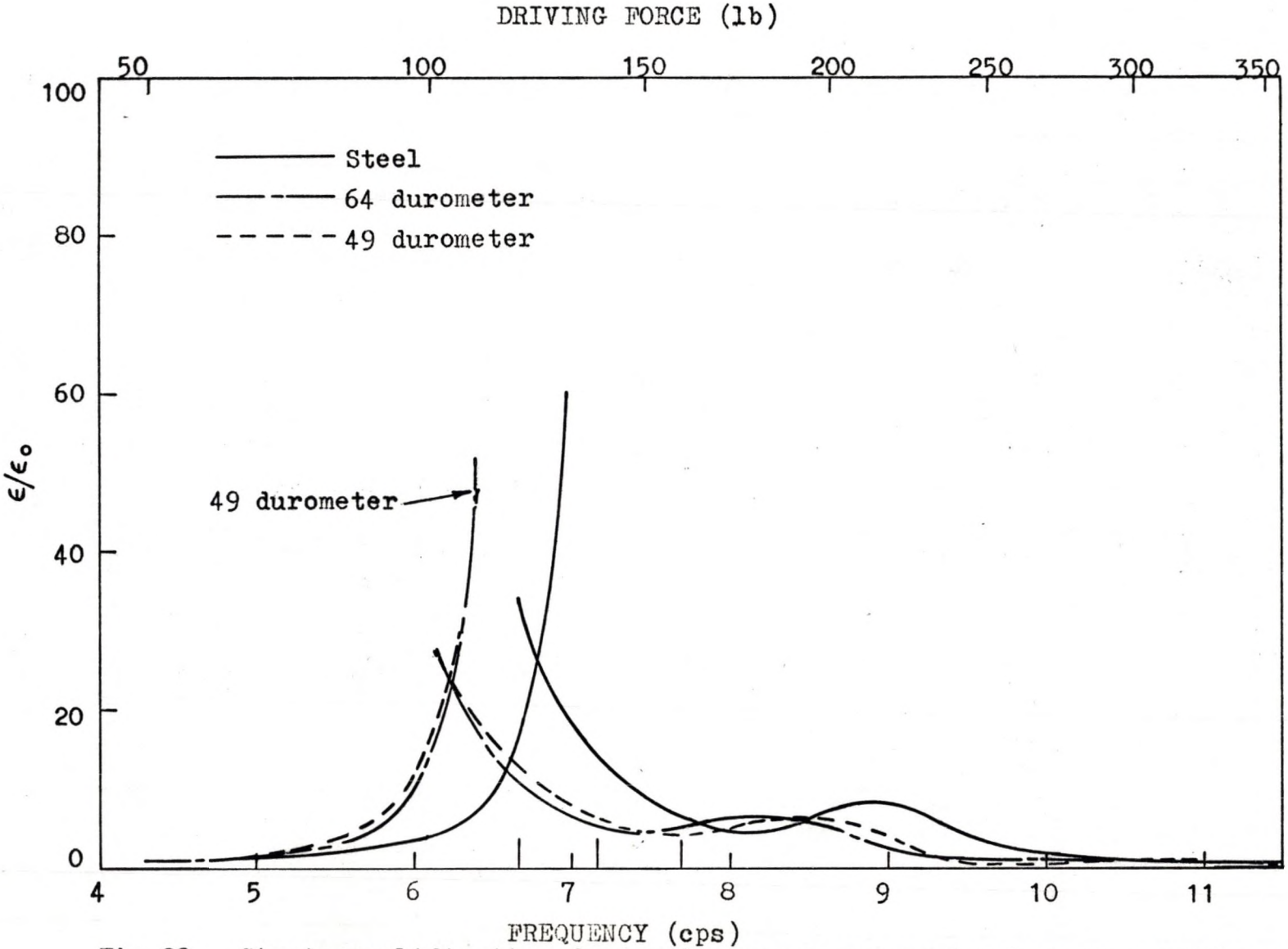

Fig.29. Strain amplification factor-frequency curves for beam B, oscillator with concrete blocks

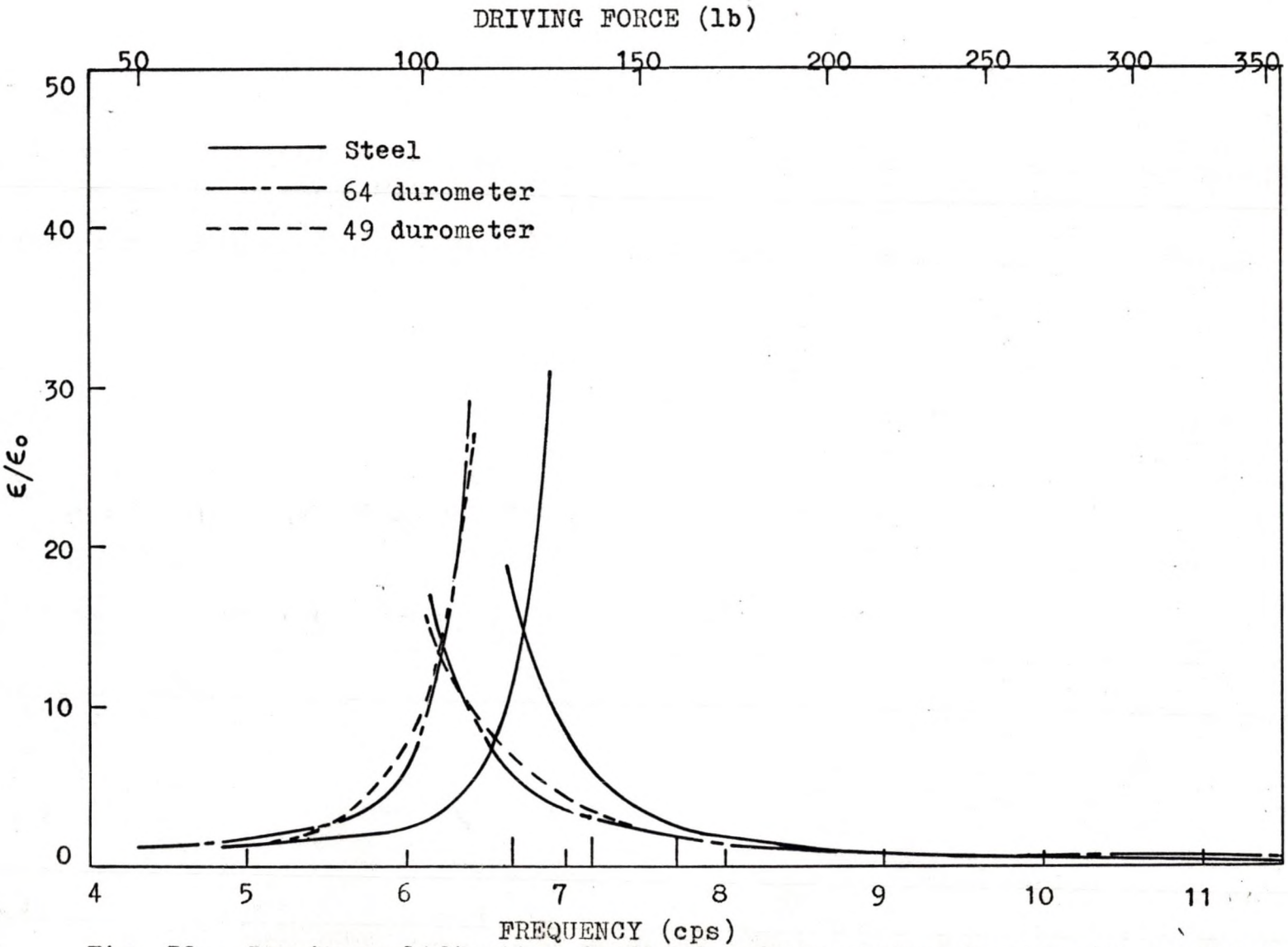

Fig. 30. Strain amplification factor-frequency curves for beam C, oscillator with concrete blocks

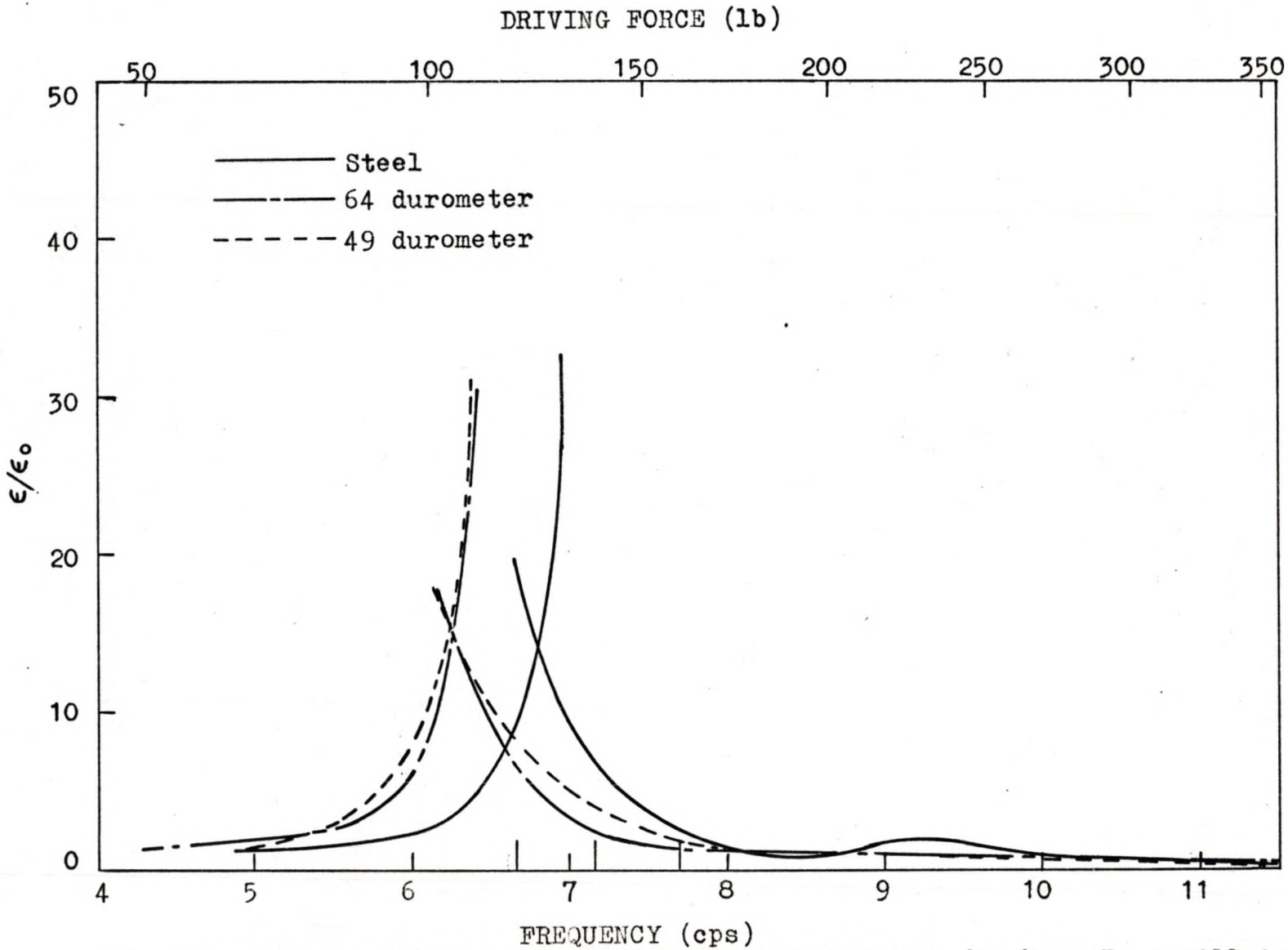

Fig. 31. Strain amplification factor-frequency curves for beam D, oscillator with concrete blocks

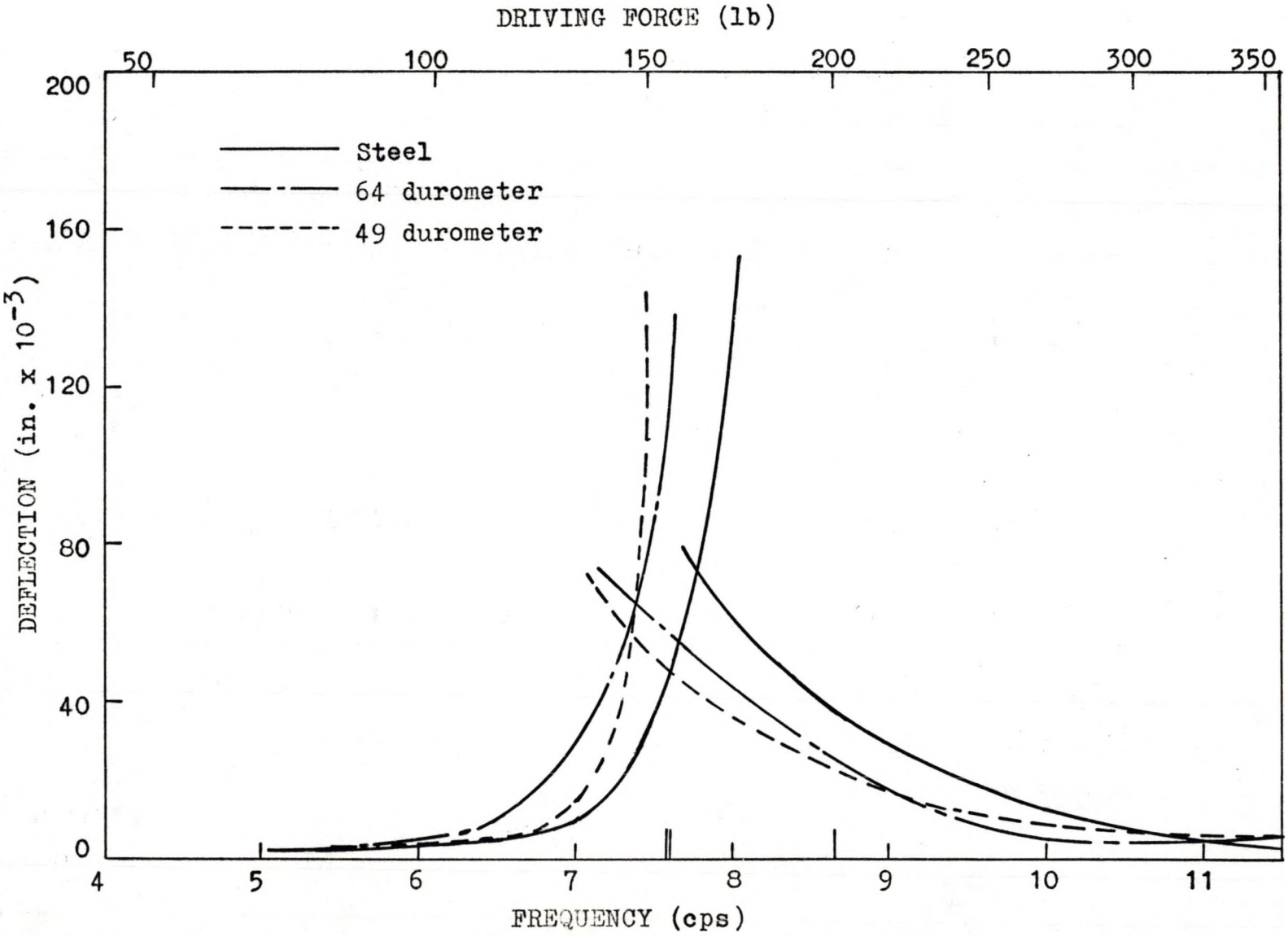

Fig. 32. Deflection-frequency curves for beam 2-1, oscillator only

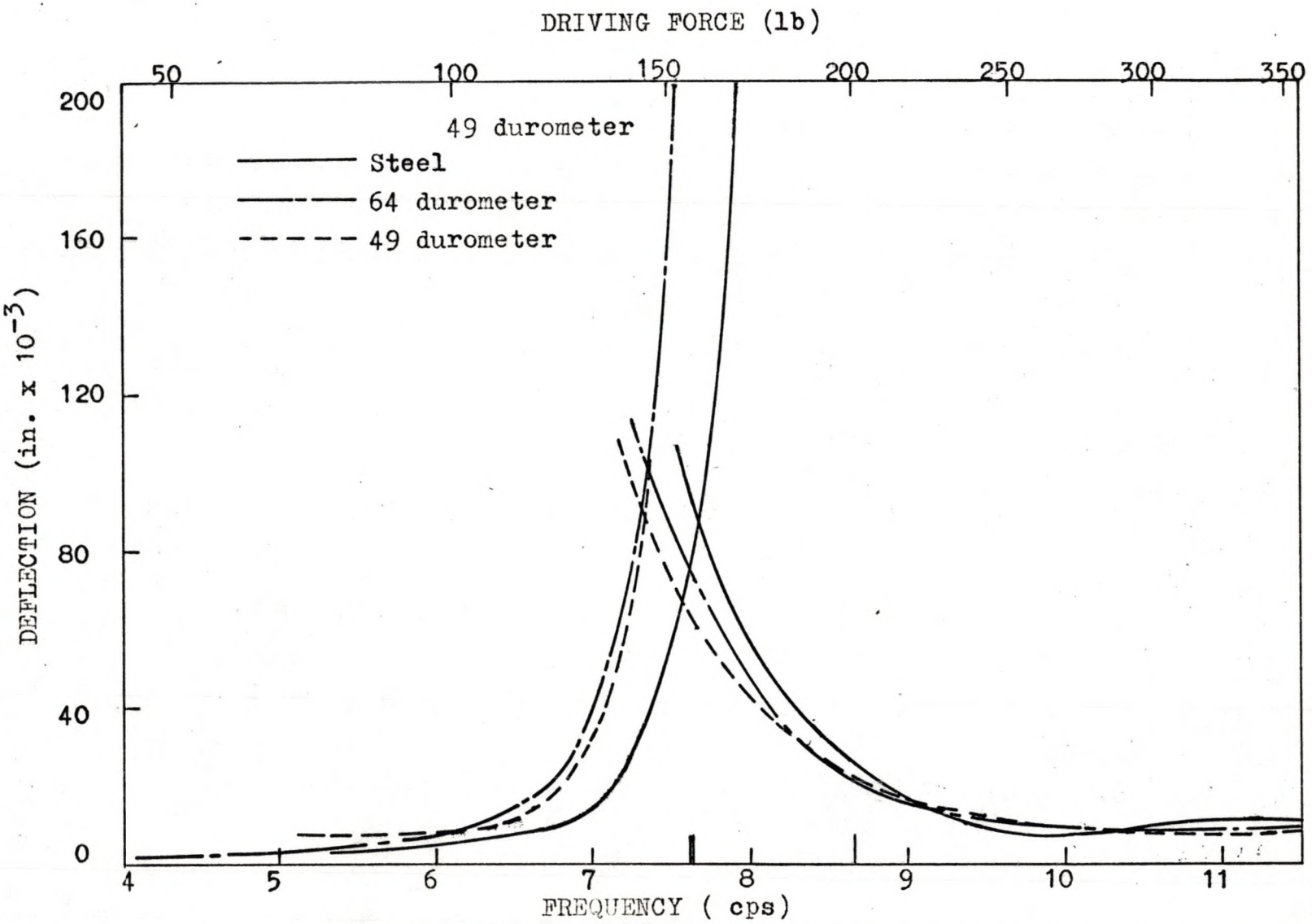

Fig. 33. Deflection-frequency curves for beam 3-1, oscillator only

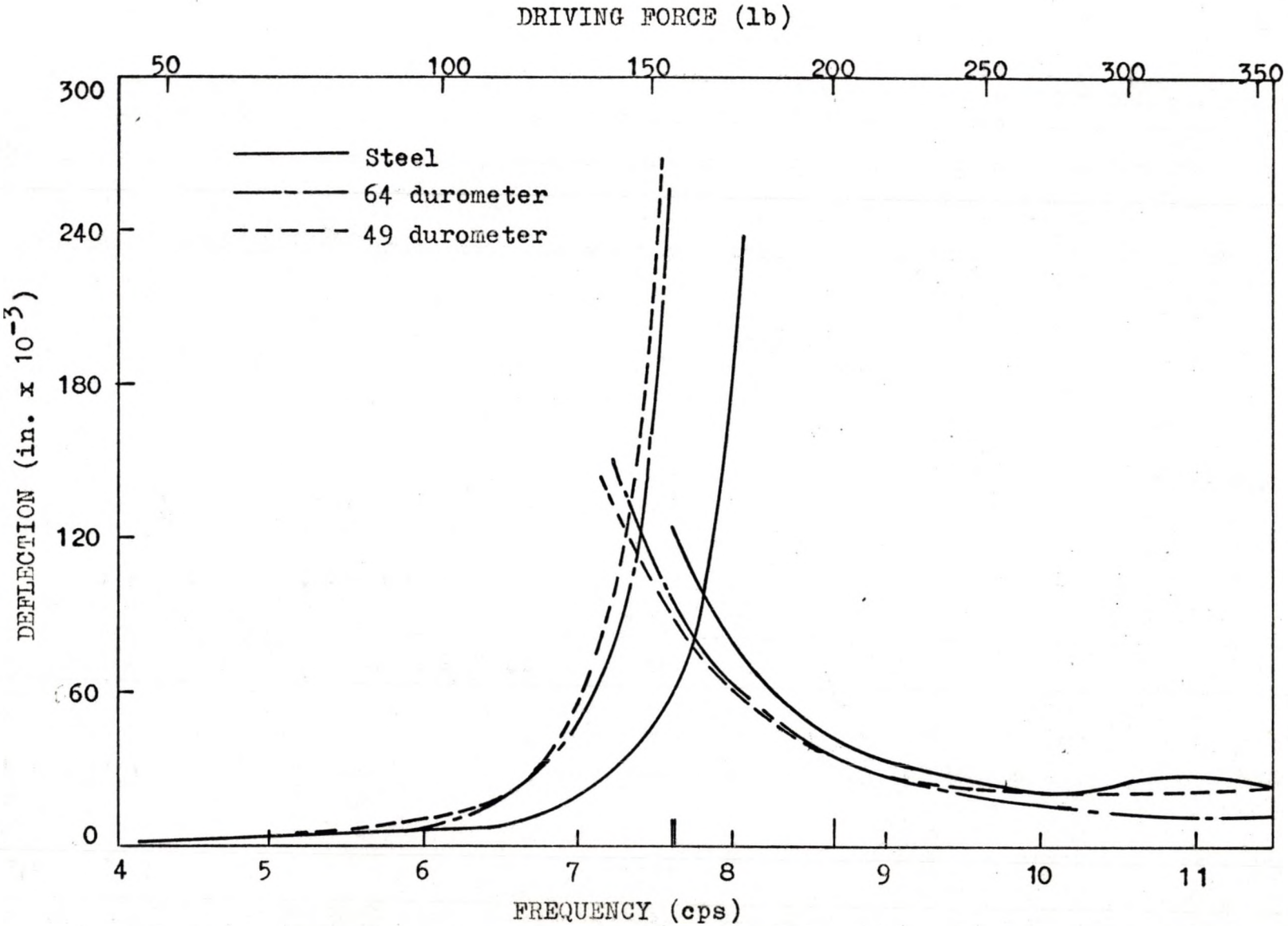

Fig. 34. Deflection-frequency curves for beam 4-1, oscillator only

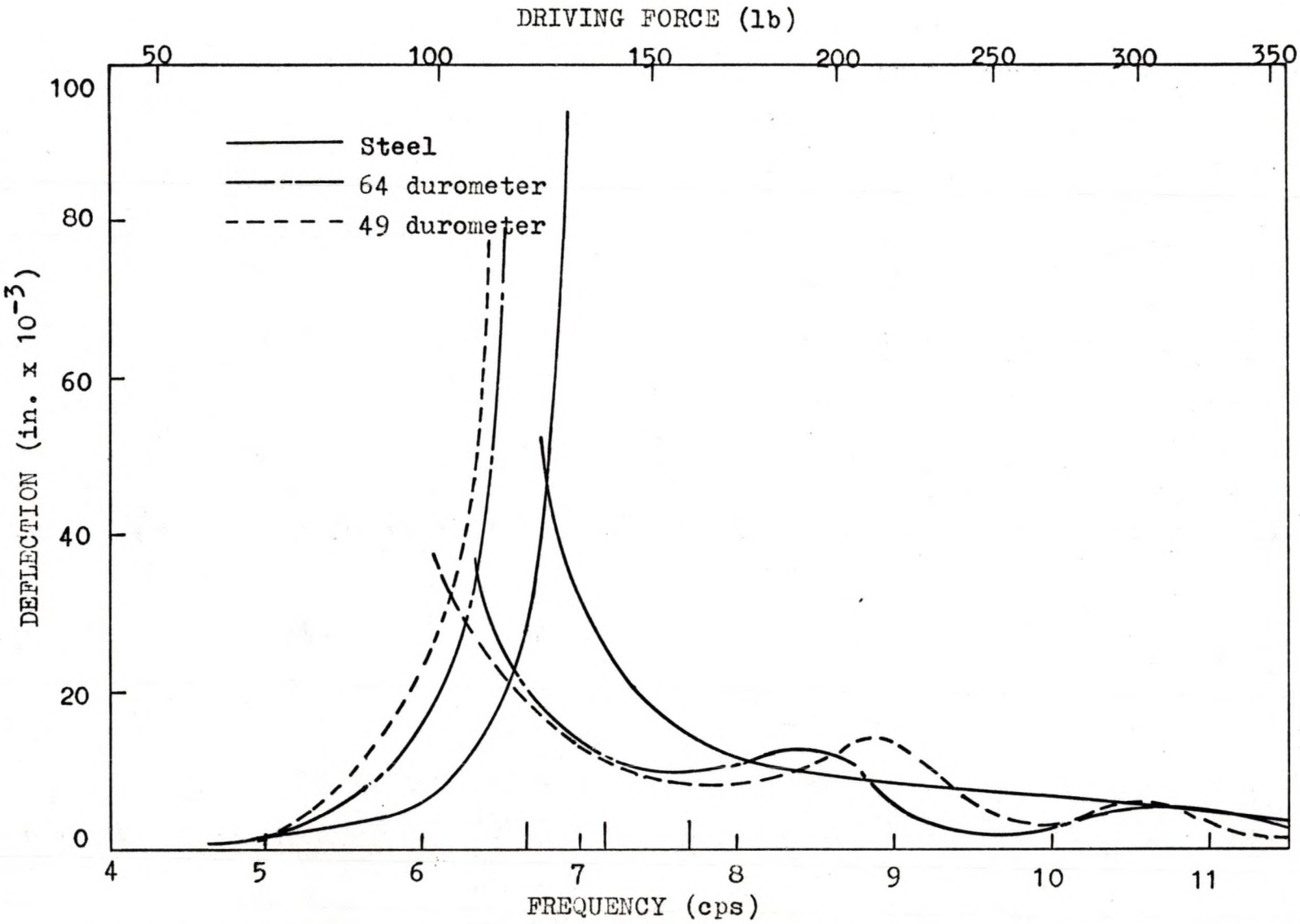

Fig. 35. Deflection-frequency curves for beam 2-1, oscillator with concrete blocks

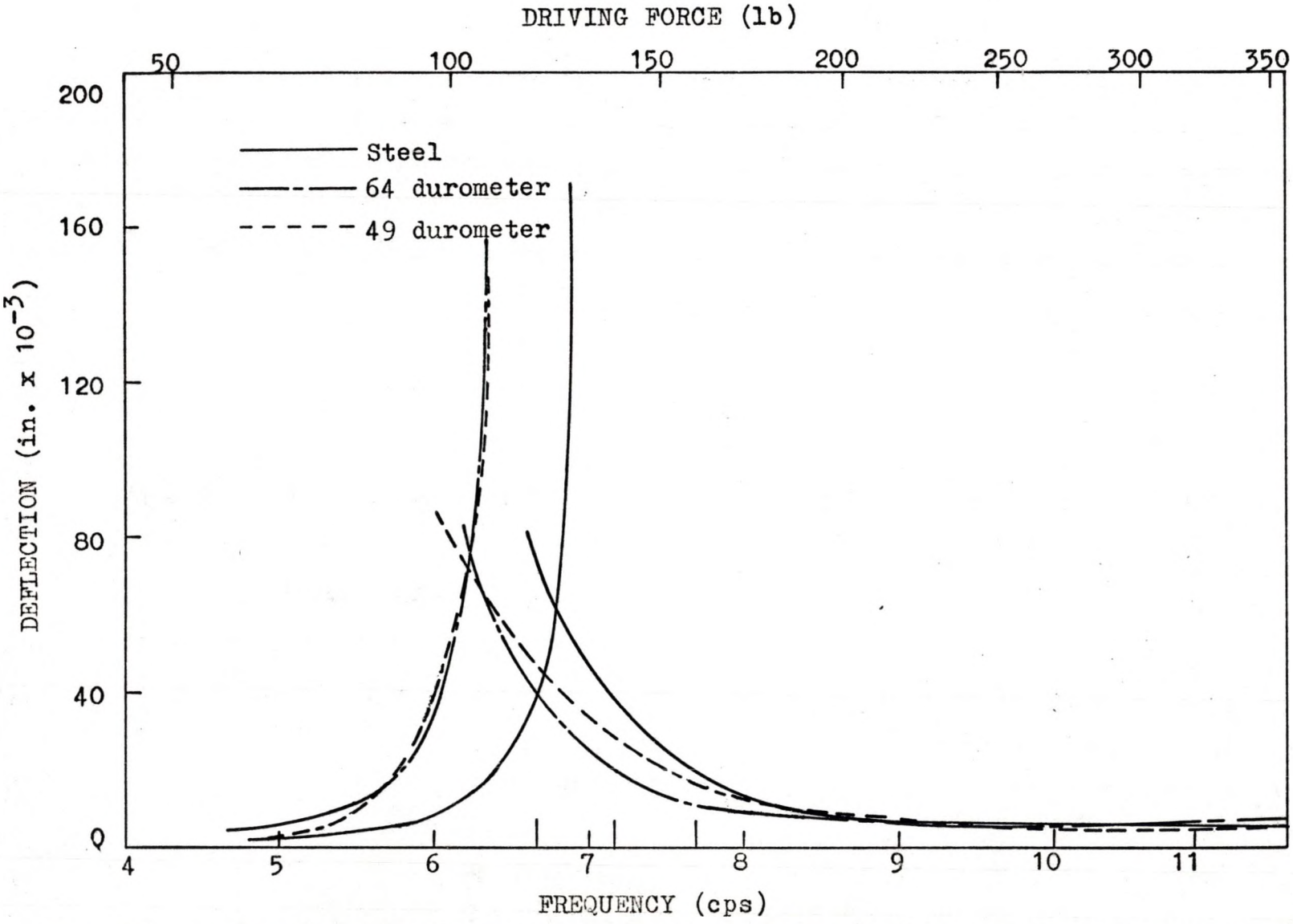

Fig. 36. Deflection-frequency curves for beam 3-1, oscillator with concrete blocks

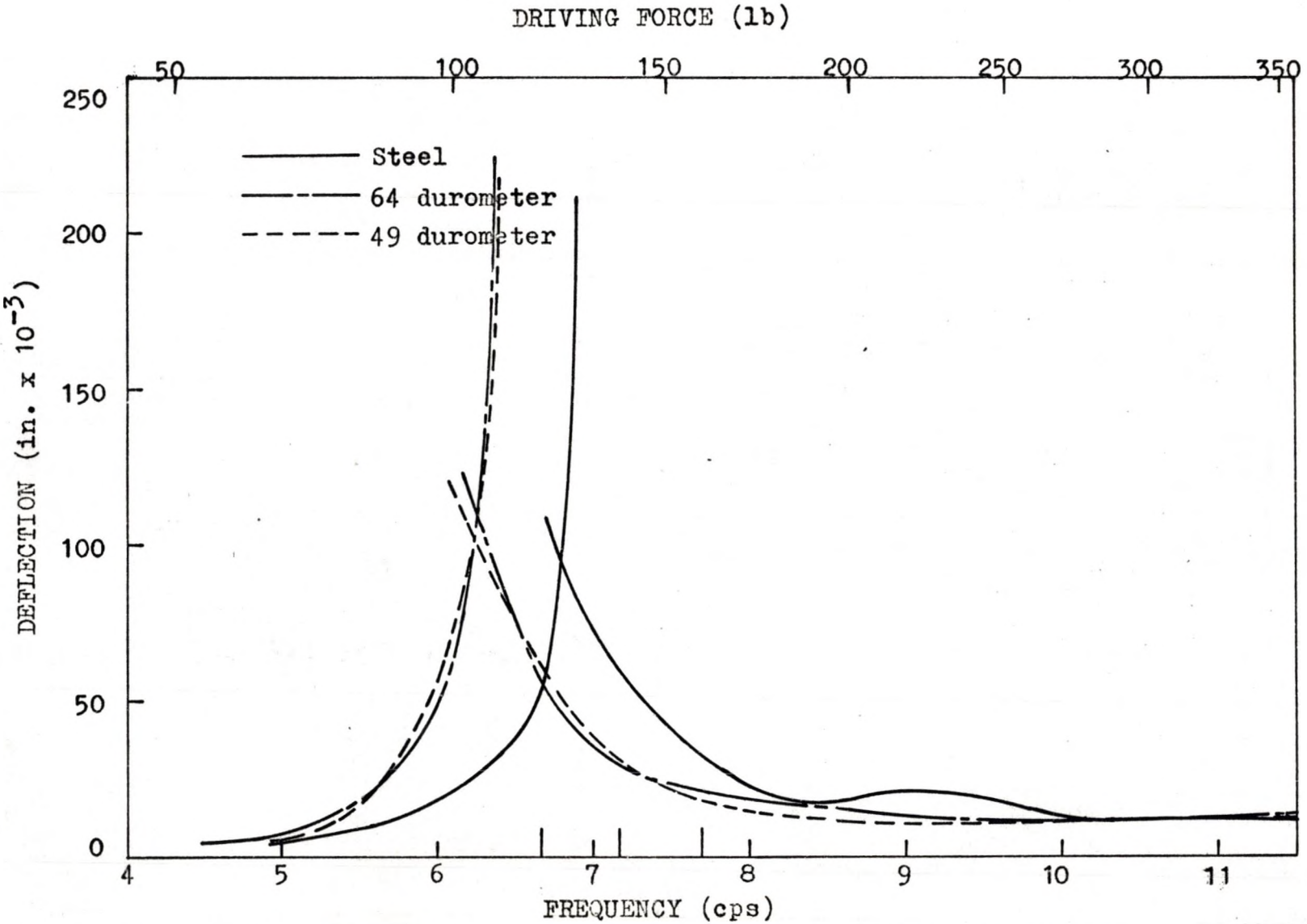

Fig. 37. Deflection-frequency curves for beam 4-1, oscillator with concrete blocks

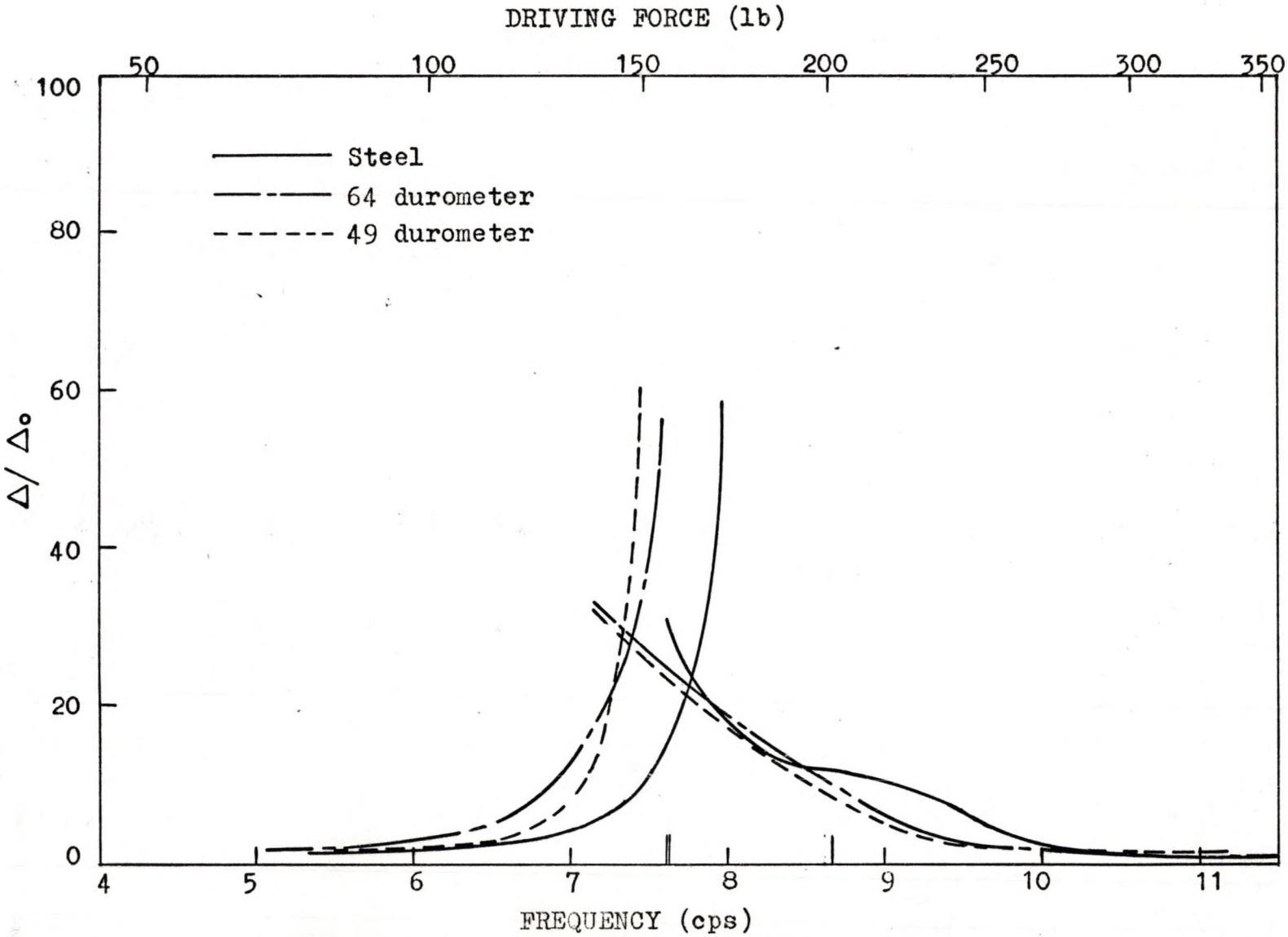

Fig. 38. Deflection amplification factor-frequency curves for beam 2-1, oscillator only

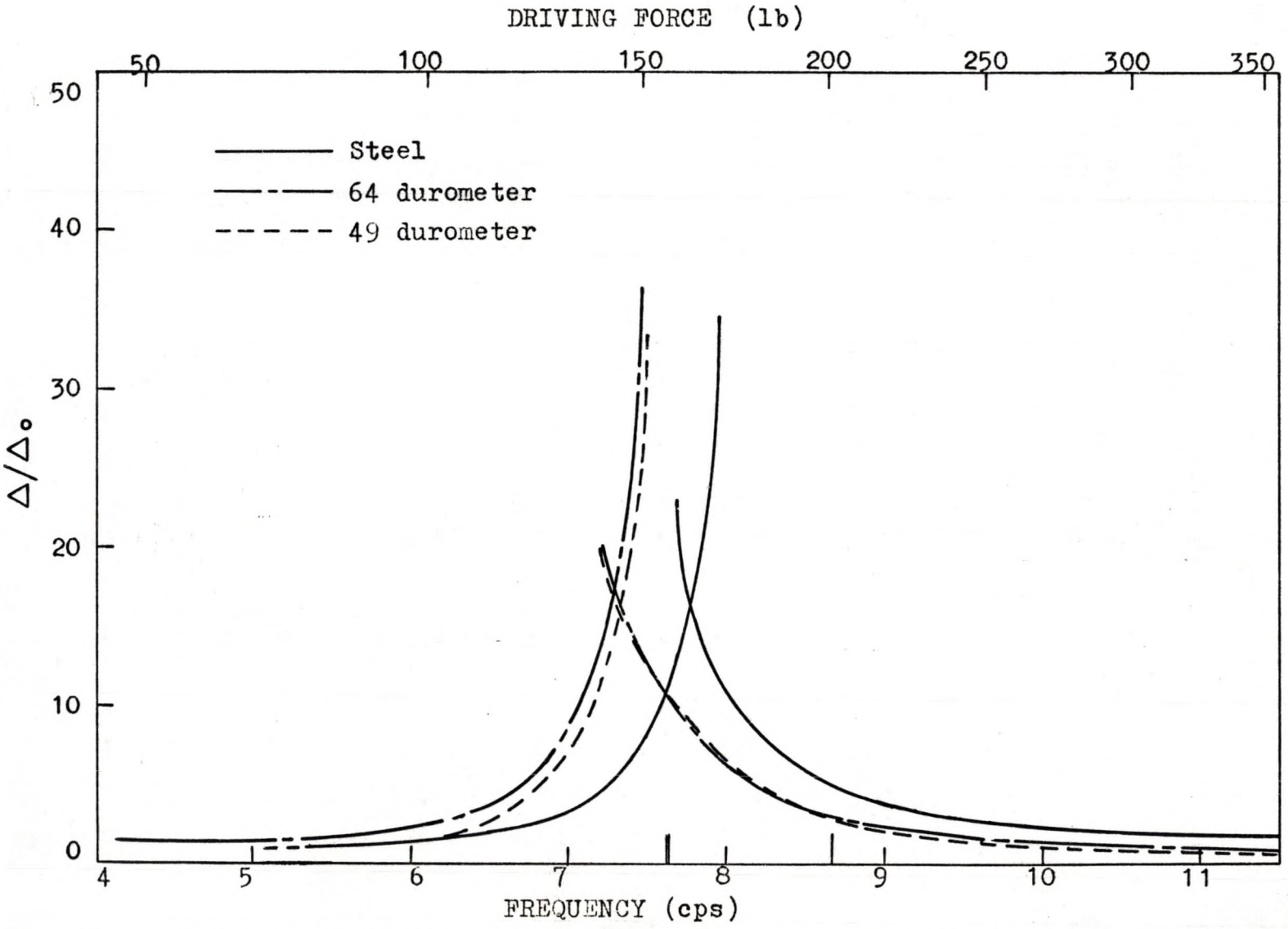

Fig. 39. Deflection amplification factor-frequency curves for beam 3-1, oscillator only

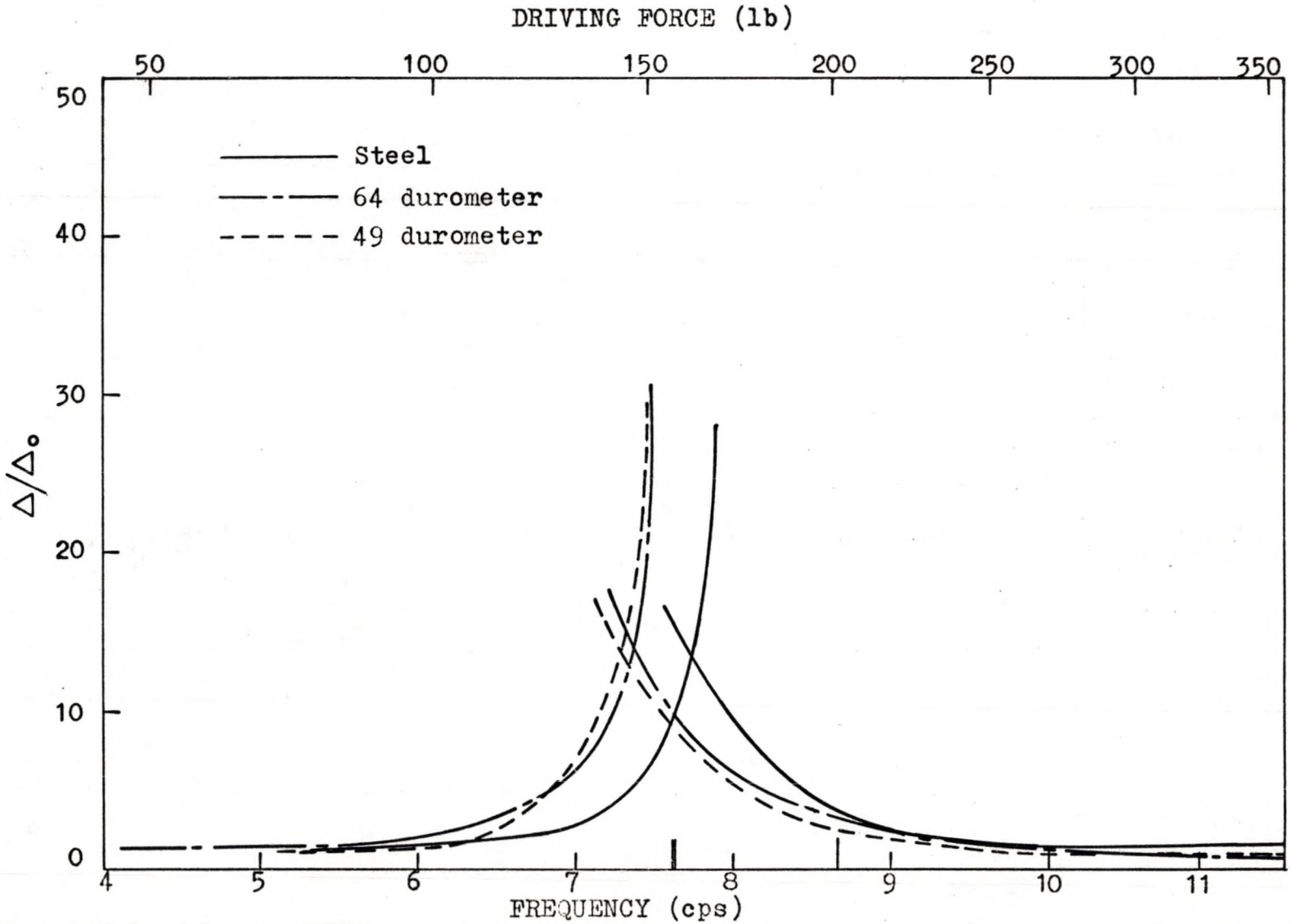

Fig. 40. Deflection amplification factor-frequency curves for beam 4-1, oscillator only

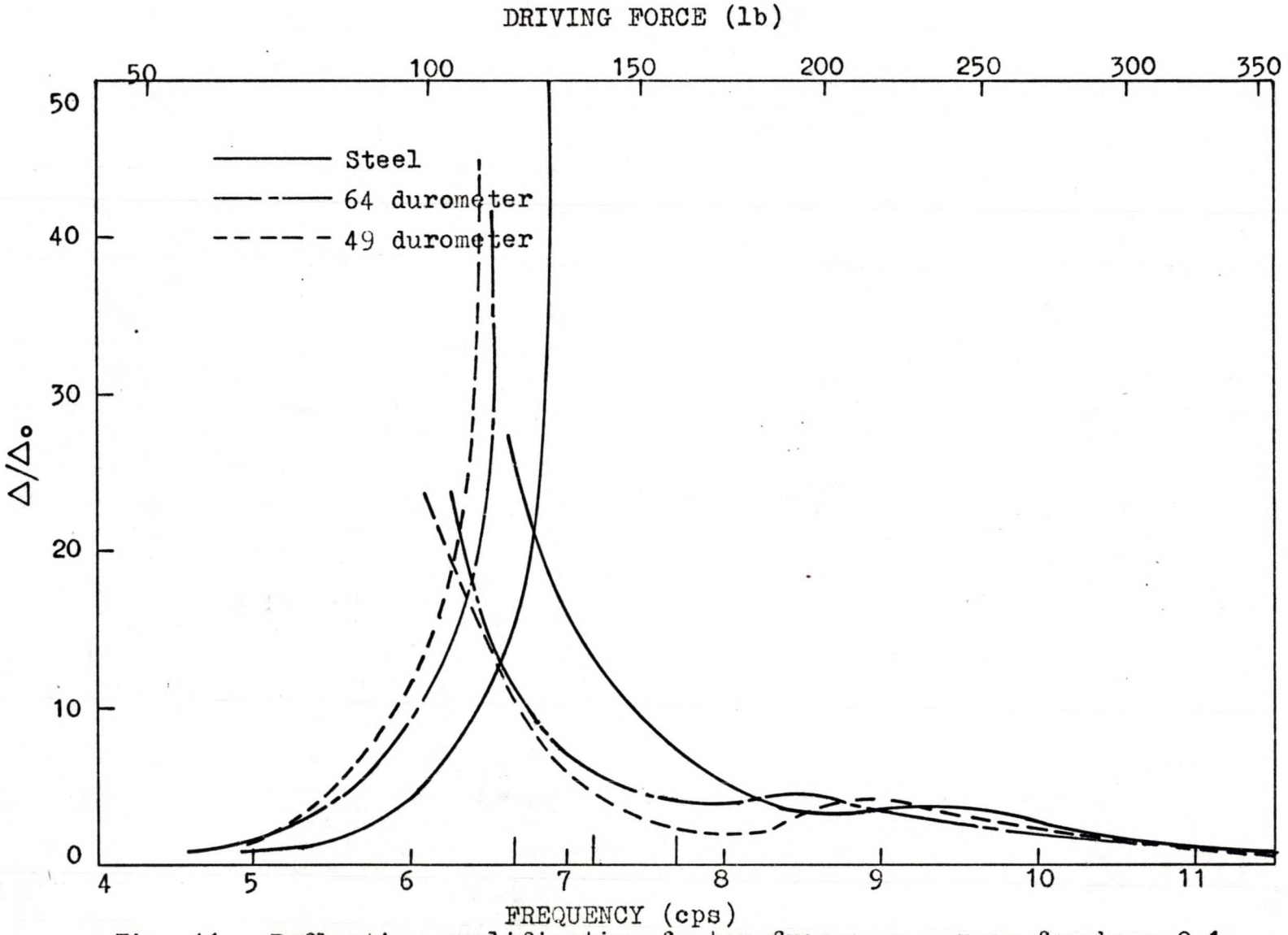

Fig. 41. Deflection amplification factor-frequency curves for beam 2-1, oscillator with concrete blocks

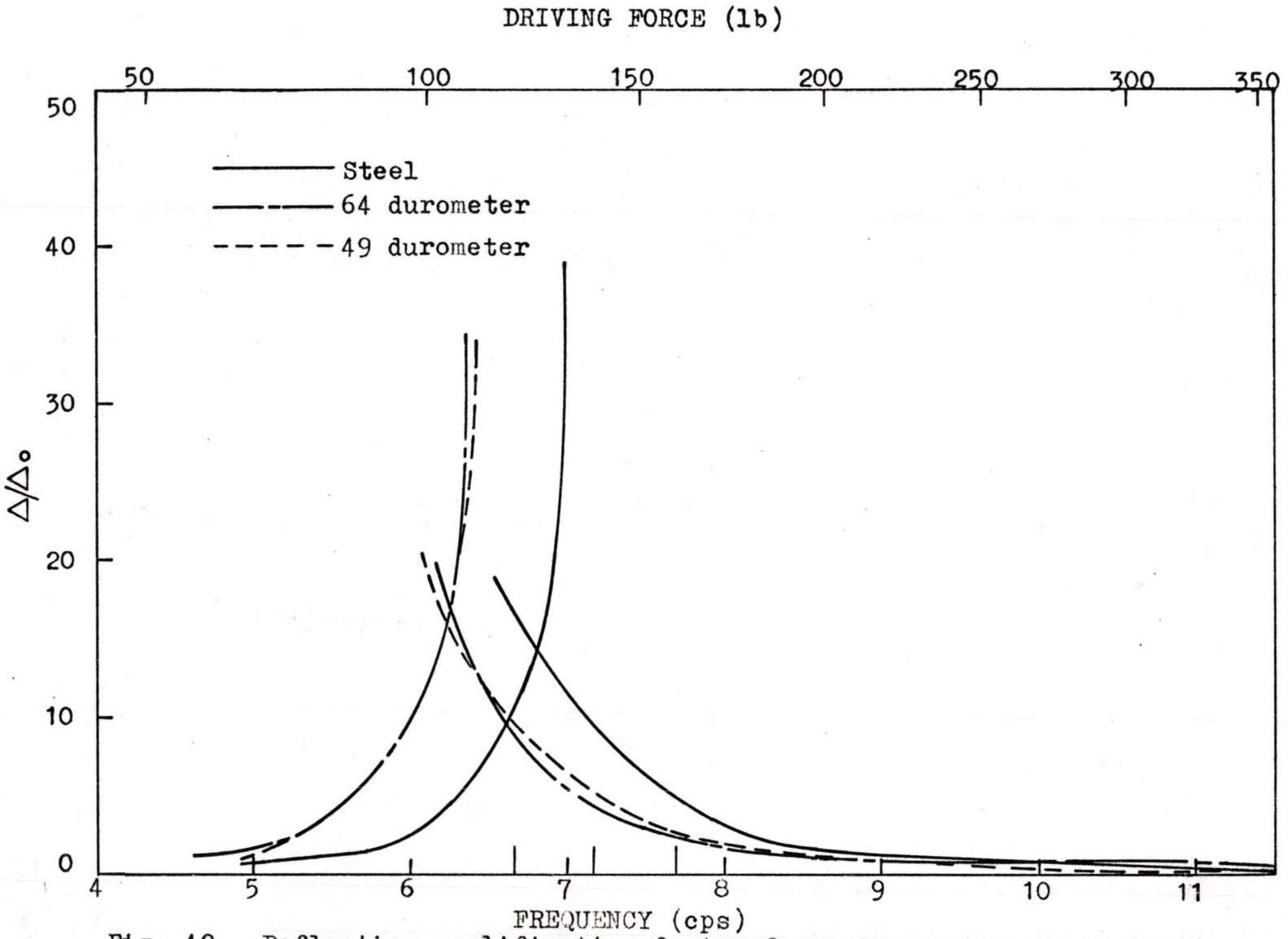

Fig. 42. Deflection amplification factor-frequency curves for beam 3-1, oscillator with concrete blocks

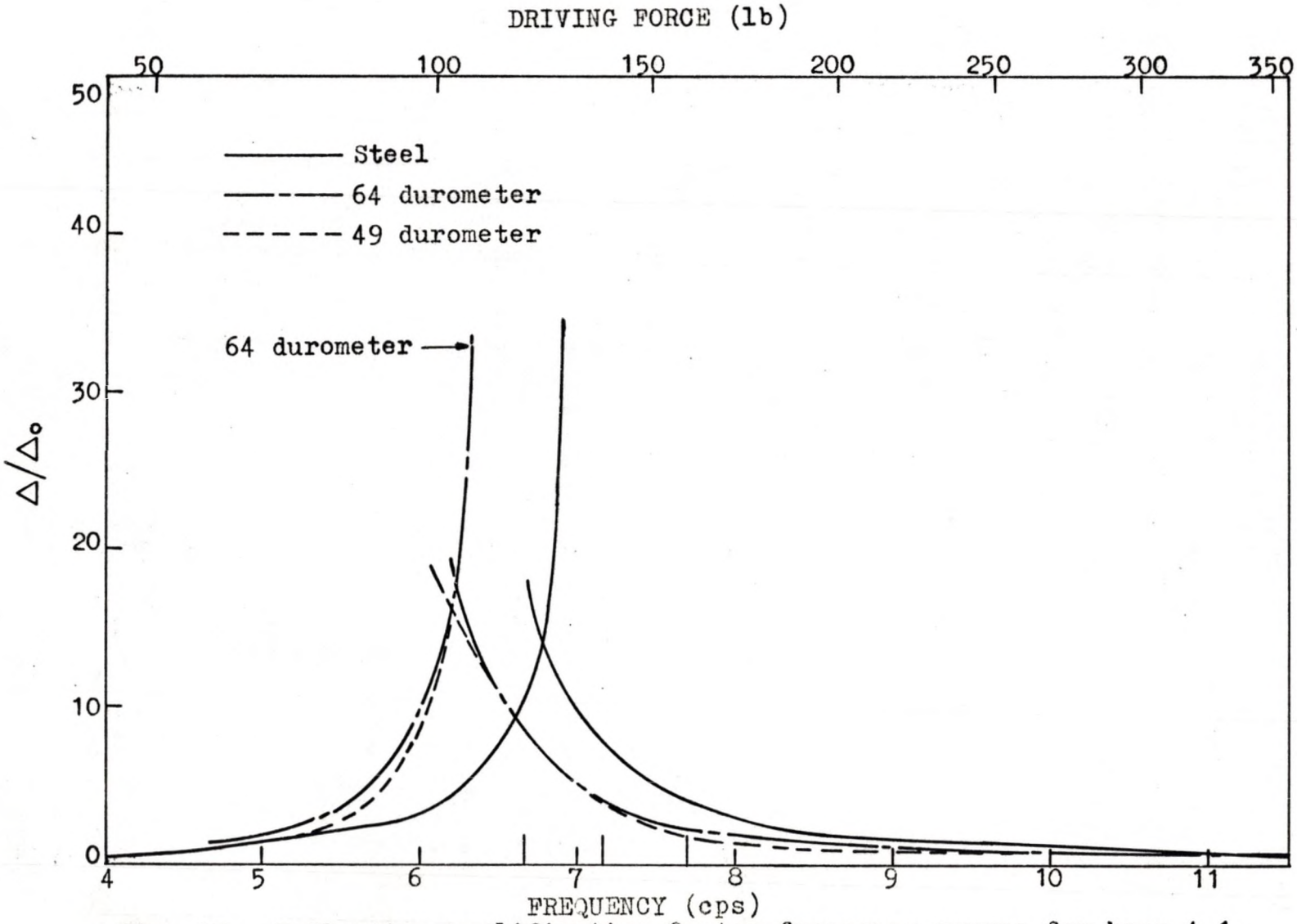

Fig. 43. Deflection amplification factor-frequency curves for beam 4-1, oscillator with concrete blocks